



Electrocoagulation as a tertiary treatment of  
municipal wastewater: Removal of enteric  
pathogen indicators and antibiotic-resistant  
bacteria

MSc thesis

Shreya Ajith Trikannad

# Electrocoagulation as a tertiary treatment for municipal wastewater: Removal of enteric pathogen indicators and antibiotic-resistant bacteria

by

**Shreya Ajith Trikannad**

**4729439**

*in partial fulfilment of the requirements for the degree of*

**Master of Science in Civil Engineering**

at the Delft University of Technology

Thesis committee:

Prof. Dr. Gertjan Medema	Delft University of Technology
Dr. Ir. Doris van Halem	Delft University of Technology
Dr. Giuliana Ferrero	IHE Delft
Ir. Bruno Bicudo Perez	Delft University of Technology
Prof. Dr Ir. Merle de Kreuk	Delft University of Technology

***August 2019***

# Acknowledgements

The past nine months have been full of challenges, immense learning and a deep sense of realization of ones privileges. This journey was made possible by a strong support system which kept on track all along.

To begin with, as we traditionally do in India, I want to start with thanking my parents. This adventurous master, so far away from home, would not have been possible without their love, sacrifice and the drive to constantly inspire me to aim higher than the sky.

Next, I would like to thank my supervisor Bruno Bicudo Perez for hearing me out and giving me critical feedback throughout the project which was very essential for it to be achievable. I thank my mentors Doris Van Halem, Gertjan Medema and Giuliana Ferrero for their constant support and encouragement. I am grateful for their valuable inputs along the way, always given at the right time to steer me through difficult waters. I have truly gained much more than academic knowledge from them and hope to have made a small space in their hearts! I thank Merle de Kreuk for providing invaluable feedback. Further, I would also like to thank Case van Genuchten who showed enthusiasm towards my project and guided me through certain aspects of my research.

I am very grateful for the help I received in the laboratory. Thank you, Mona Soliman, for guiding me throughout my research. I thank Armand Middeldorp for being ever ready to help and assist me whenever needed. I also thank Patricia van den Bos for the ICP-MS analysis and Ruud Hendrikx from the Department of Materials Science and Engineering for X-ray analysis.

In every journey friends always help you survive through the daily struggles and I am blessed with a host of them in Delft and in India alike. I am thankful to them for pulling me through my lows and applauding my highs throughout the year.

Finally, I have to thank my partner, Sachin Sathish, without whom this would have been almost impossible. He has, with utmost diligence, tolerated my various moods and constantly motivated to finish what I had started. Our journey together through this masters has enriched me and set higher ambitions for myself.

# Abstract

With the growing population and economic development, there is more stress on natural water resources. Additionally, current and future water shortages, increasing environmental concerns and stringent discharge standards demand high-quality treated water. In this scenario, it is crucial to recover water and wastewater resources for reuse, reducing the dependency on new resources. While aiming for water reclamation, the influence of wastewater quality parameters on human health is given foremost attention in recent times. Enteric pathogens are a major concern when reclaiming municipal wastewater. Electrocoagulation (EC) process that introduces coagulants by electrochemical means has been successfully employed for the treatment of groundwater, industrial and municipal wastewater. EC has been widely accepted over other physicochemical processes due to its process design and low-cost material. In this research, EC has been thoroughly investigated as a tertiary treatment technology for water reclamation from municipal wastewater.

This research is focused on determining the efficiency of low voltage iron EC for the removal of enteric pathogen indicators and antibiotic-resistant bacteria from secondary wastewater effluent. The effect of operational parameters: charge dosage (C/L) and charge dosage rate (C/L/min) on pollutant reduction was evaluated in different water matrices: demineralized water, synthetic wastewater effluent and real wastewater effluent. EC operated at 400 C/L, 7.2 C/L/min and natural pH allowed > 3.5 log units removal for *E. coli* and Enterococci, > 2.5 log units for *ESBL E. coli* and VRE and > 2 and 2.7 log units for Somatic coliphages and *Clostridium perfringens* spores respectively in real wastewater effluent. Furthermore, a significant reduction of phosphorous, COD and true color was observed at 400 C/L and 36 C/L/min. Pollutant reduction was influenced by sedimentation and floatation mechanisms observed at varying charge dosage rates.

A marginally higher removal rate constant of pathogen indicators as a function of charge dosage at low charge dosage rate showed slow iron dosing to improve microbial adsorption and increase contact time with iron precipitates. The reduction of pathogen indicators was associated with physical removal mechanisms like adsorption, sweep coagulation and entrapment within the flocs, charge neutralization and aggregation based on literature. The effective removal of physical, chemical and microbiological parameters in real wastewater effluent was achieved at 400 C/L and 7.2 C/L/min at an operating cost of 0.17 €/m<sup>3</sup> indicating EC to be a cost-effective treatment in comparison to alternative technologies like ozone, UV, activated carbon and reverse osmosis.

# Table of Contents

Abstract.....	IV
List of Figures.....	VII
List of Tables.....	IX
Symbols and Abbreviations.....	X
<b>1. Introduction.....</b>	<b>1</b>
1.1 Background.....	1
1.2 Problem statement.....	3
1.3 Research question and objectives.....	4
1.3.1 Research question.....	4
1.3.2 Hypothesis.....	4
1.3.3 Goals and objectives.....	5
<b>2. Literature review.....</b>	<b>6</b>
2.1 Pathogens in municipal wastewater.....	6
2.1.1 Bacteria.....	7
2.1.2 Viruses.....	7
2.1.3 Protozoa.....	7
2.1.4 Antibiotic-resistant bacteria.....	8
2.2 Theory of electrocoagulation.....	9
2.2.1 Reaction at electrodes.....	10
2.3 Electrocoagulation for wastewater disinfection.....	13
2.4 Effect of operational parameters.....	14
2.4.1 Electrode material.....	14
2.4.2 Initial pH.....	14
2.4.3 Electrocoagulation time.....	15
2.4.4 Charge dosage.....	15
2.4.5 Charge dosage rate.....	16
2.4.6 Electrode arrangements.....	17
2.4.7 Inter-electrode distance.....	18
2.4.8 Surface area to volume ratio.....	18
2.4.9 Stirring speed.....	18
2.5 Pollutant removal mechanisms.....	19
2.5.1 Microorganisms.....	20
2.5.2 Wastewater quality parameters.....	21
<b>3. Materials and Methods.....</b>	<b>24</b>
3.1 Experimental setup.....	24
3.2 Wastewater composition.....	25
3.3 Preparation of microbiological cultures.....	27
3.3.1 Preparation of <i>WRI E. coli</i> Stock culture.....	27
3.3.2 Preparation of stock cultures of somatic coliphage bacterial host <i>E. coli</i> WG5 (ATCC 700078).....	27

3.3.3 Preparation of working cultures of somatic coliphage bacterial host <i>E. coli</i> WG5 (ATCC 700078) .....	28
3.3.4 Calibration curve of somatic coliphage bacterial host <i>E. coli</i> WG5 (ATCC 700078) .....	28
3.3.5 Preparation of Coliphage $\phi$ X174 stock .....	28
3.4 Procedure for microbiological assays .....	29
3.4.1 Bacterial assays .....	29
3.4.2 Somatic coliphage assay .....	29
3.4.3 <i>Clostridium perfringens</i> spore assay .....	30
3.5 Physical and chemical analysis .....	31
3.6 Electrocoagulation experiments .....	31
3.6.1 Experimental procedure .....	32
3.6.2 Summary of experimental conditions .....	33
3.7 Treatment cost .....	35
<b>4. Results .....</b>	<b>36</b>
4.1 Evolution of pH .....	36
4.2 Iron dissolution .....	37
4.3 Effect of current density .....	38
4.4 Effect of charge dosage and charge dosage rate (CDR) on microbial attenuation .....	39
4.4.1 Demineralized water .....	39
4.4.2 Synthetic wastewater effluent .....	40
4.4.3 Municipal wastewater effluent .....	41
4.5 Removal of wastewater quality parameters .....	43
4.5.1 Synthetic municipal wastewater effluent .....	44
4.5.2 Municipal wastewater effluent .....	46
4.6 Sludge characterisation .....	51
4.7 Removal kinetics of pathogen indicators .....	52
4.8 Operating cost analysis .....	55
4.9 Comparison of EC effluent with reclaimed water quality standards .....	54
<b>5. Discussion .....</b>	<b>57</b>
5.1 pH increase during electrocoagulation .....	57
5.2 Reason for a high Faradic Efficiency .....	57
5.3 Influence of charge dosage rate .....	58
5.4 Proposed removal mechanisms for enteric pathogens indicators and ARB .....	59
5.5 Proposed removal mechanisms for wastewater quality parameters .....	62
5.6 Inactivation kinetics .....	63
<b>6. Conclusion .....</b>	<b>64</b>
<b>7. Recommendations .....</b>	<b>66</b>
<b>8. References .....</b>	<b>67</b>

## List of figures

Figure 1	Electrochemical reactions during electrocoagulation process.....	9
Figure 2	Coagulation and flocculation stages during electrocoagulation.....	10
Figure 3	Predominance zone diagram for iron species as a function of pH.....	11
Figure 4	Electrode arrangements in electrocoagulation reactor.....	17
Figure 5	Important mechanisms of pollutants removal by electrocoagulation.....	19
Figure 6	Experimental setup for electrocoagulation experiments.....	24
Figure 7	Iron plates used as electrodes for EC experiments.....	25
Figure 8	Calibration curve of somatic coliphages bacterial host E. coli WG5.....	28
Figure 9	Identification of different pathogen indicators.....	31
Figure 10	Three sets of samples collected before and after EC.....	32
Figure 11	Final pH in demineralized water.....	36
Figure 12	Final pH in synthetic wastewater effluent.....	37
Figure 13	Final pH in real wastewater effluent.....	37
Figure 14	Iron concentration in bulk and supernatant of real wastewater effluent.....	38
Figure 15	Iron precipitates a) before flocculation and b) after flocculation.....	38
Figure 16	Effect of current density on WR1 E. coli removal in synthetic wastewater effluent.....	39
Figure 17	Removal of WR1 E. coli (a) and $\phi$ X174 Somatic coliphages in demineralized water.....	39
Figure 18	Removal of WR1 E. coli in synthetic municipal wastewater effluent.....	40
Figure 19	Removal of $\phi$ X174 Somatic coliphages in synthetic municipal wastewater effluent.....	41
Figure 20	Removal of E. coli, ESBL E. coli, Enterococci and VRE in real wastewater effluent at 7.2 C/L/min.....	41
Figure 21	Removal of E. coli, ESBL E. coli, Enterococci and VRE in real wastewater effluent at 36 C/L/min.....	42
Figure 22	Removal of somatic coliphages in real wastewater effluent.....	42
Figure 23	Removal of C. perfringens spores in real wastewater effluent.....	43
Figure 24	Phosphorous removal in synthetic wastewater effluent (experiment 1).....	43

Figure 25	Phosphorous removal in synthetic wastewater effluent (experiment 2).....	44
Figure 26	Total nitrogen removal in synthetic wastewater effluent (experiment-1).....	44
Figure 27	Total nitrogen removal in synthetic wastewater effluent (experiment-2).....	45
Figure 28	Phosphorous removal in real wastewater effluent.....	45
Figure 29	Total nitrogen removal in real wastewater effluent.....	46
Figure 30	NO <sub>3</sub> <sup>-</sup> , NO <sub>2</sub> <sup>-</sup> and NH <sub>4</sub> <sup>+</sup> conversions in real wastewater effluent.....	46
Figure 31	Organic and inorganic N removal in municipal wastewater effluent.....	47
Figure 32	Reduction in COD concentration (a) and removal percentage (b) in real wastewater effluent.....	47
Figure 33	TSS variation in real wastewater effluent.....	48
Figure 34	Turbidity variation in real wastewater effluent.....	48
Figure 35	True color removal in real wastewater effluent.....	49
Figure 36	Flocs sedimentation (a) floatation (b) and formation of bubbles (C) in synthetic wastewater effluent.....	50
Figure 37	Nature of iron precipitates in synthetic wastewater effluent.....	51
Figure 38	Characterization of EC sludge in real wastewater effluent.....	51
Figure 39	Log-linear relation between E.coli removal and charge dosage.....	51
Figure 40	Log-linear relation between C. perfringens spores removal and charge dosage..	52
Figure 41	Log-linear relation between Somatic coliphages removal and charge dosage.....	52

## List of Tables

Table 1.	Composition of synthetic municipal wastewater effluent .....	26
Table 2.	Characteristics of real municipal wastewater treatment effluent.....	26
Table 3.	Specific culture mediums and incubating conditions for different pathogen indicators.....	29
Table 4.	Operational parameters for phase 1 experiments.....	33
Table 5.	Operational parameters for phase2 experiments.....	34
Table 6.	Operational parameters for phase 3 experiments.....	34
Table 7.	Theoretical and experimental Fe concentration as a function of charge dosage.....	38
Table 8.	Parameters of log-linear model for removal kinetics of pathogen indicators.....	54
Table 9.	Operating cost at different charge dosages and CDRs.....	55
Table 10.	Comparison of EC effluent with reclaimed water quality guidelines.....	56

## Symbols and Abbreviations

<b>ARB</b>	Antibiotic-Resistant Bacteria
<b>AS</b>	Activated sludge
<b>CDR</b>	Charge dosage rate
<b><math>C_{energy}</math></b>	Electrical energy cost
<b><math>C_{electrode}</math></b>	Electrode material cost
<b>EC</b>	Electrocoagulation
<b>EU</b>	European Union
<b><math>Fe_{exp}</math></b>	Experimentally determined iron concentration
<b><math>Fe_{theo}</math></b>	Theoretical iron concentration
<b>Fe-EC</b>	Iron electrocoagulation
<b>k</b>	Removal rate constant
<b>TN</b>	Total nitrogen
<b>US EPA</b>	United States Environmental Protection Agency
<b>VRE</b>	Vancomycin-Resistant Enterococci

# Chapter-1

## Introduction

### 1.1 Background

Water scarcity and shortage of safe drinking water are among the most serious challenges of the 21<sup>st</sup> century. Water resources are irregularly distributed in space and time and are under pressure due to human activities and economic development. Fast-tracked urbanization and increase of municipal water supply and sanitation systems contribute to the rising demand. Additionally, climate change scenarios, spatial and temporal variations of water cycle dynamics intensify the discrepancies between water supply and demand (Voulvoulis, 2018). At present, one-third of the world's population lives in water-stressed countries and, by 2025 the figure is expected to rise to two-thirds (Elimelech, 2006).

The availability of water resources is intrinsically associated with water quality, as pollution of water sources may restrict different types of uses. Discharge of untreated wastewater into the water sources can degrade water quality, increasing the risk of human health and ecosystem. This trend, if persists can lead to water scarcity and constrain sustainable economic development (Voulvoulis, 2018).

As economic development rises, freshwater supplies become more limited. Water reuse is often recognised as a solution with great potential in reducing the gap between availability and demand. Research evidence demonstrates the safety of potable reclaimed water and the successful implementation of water recycling schemes in countries like Singapore and Namibia (Fielding et al., 2017). Likewise, direct and indirect potable reuse is not practised in many countries due to public acceptance. However, in recent times reclaimed water use is extensively encouraged for activities such as irrigation, groundwater recharge and domestic use (Levine and Asano, 2004). The 2030 agenda for Sustainable Development Goals targets improvement in water quality by reducing pollution, eliminating the discharge of polluted waters, halving the proportion of untreated wastewater and increase safe water reuse globally (Estrada et al., 2017).

While aiming for water reclamation, the impact of wastewater quality parameters on intended applications must be considered, mainly its influence on human health and the ecosystem. Wastewater

harbours a wide range of enteric pathogens such as virus, bacteria, protozoa, parasitic worms and eggs. Urban effluent reaching a conventional wastewater treatment plant typically passes through primary and secondary treatment step. A biological process such as activated sludge (AS) is the most widely used secondary treatment. AS is observed to reduce pathogen concentrations only to a certain degree (1-3 log units) (Chahal et al., 2016); the effectiveness of removal is much higher for bacteria than viruses which are smaller in size, simpler in structure and more persistent in the environment. As a result, municipal wastewater treatment plants serve as major sources of enteric pathogens, antibiotic-resistant bacteria and genes (Michael et al., 2013).

The required level of pathogen reduction in reclaimed water depends on the nature of reuse application and potential for human or stock exposure to water. A tertiary or advanced treatment step like disinfection is specifically designed for the reduction of pathogen numbers to levels that meet public health safety requirements. The suitable technology is evaluated based on common indices such as system reliability, ease of operation, capital cost, ability to remove pathogenic microorganisms, environmental impacts and additional treatments. Chlorination, UV, ozonation, membrane filtration and natural treatment are the most common disinfection systems used in water reclamation. Chlorination is widely used worldwide due to its strong disinfection capability and low cost, but the drawback is the formation of undesirable disinfection byproducts and resistance of few potential pathogens to treatment. Alternatives such as UV, ozonation and membrane filtration are effective but are not practical for treating large volumes of wastewater due to high cost and maintenance.

The need for effective and economical alternatives has led to the development of electrochemical disinfection, of which electrocoagulation (EC) and electro-Fenton are the most promising technologies. Electrocoagulation is a physicochemical phenomenon where a sacrificial metallic anode releases metal ions and cathode produces hydroxyl ions and hydrogen gas. These metal ions are hydrolysed to form respective hydroxides which are excellent coagulants. These coagulants destabilize pollutants by various mechanisms which allow pollutants to adsorb or encapsulate onto hydroxide's active surfaces (Garcia-Segura et al., 2017).

Previous studies have demonstrated the effect of EC in the removal of a wide range of microorganisms from bacteria to viruses in different water matrices (Delaire et al., 2016; Estrada et al., 2017, Pulido, 2005). The main advantage of this process is the production of disincentive conditions in situ in the treatment device, thus avoiding transport, storage and handling of disinfectants/equipment.

## 1.2 Problem statement

Discharge or reuse of secondary treated effluent with active pathogens increases the risk for human health. For safe reuse applications which involve high risk of human exposure, the water quality demands *E. coli* level to be less than 10 cfu/100 ml. The concentration can be less than 100 cfu/100 ml when there is a medium risk of human or specified livestock contact (Victoria, 2002) (Alcalde-Sanz and Gawlik, 2017). Water quality assessment of a secondary treatment effluent of a conventional Dutch wastewater treatment plant with AS showed *E. coli* concentration in the range of  $10^4$ - $10^5$  cfu/100 ml. This evaluation convinces that primary and secondary processes do not ensure adequate removal of pathogen indicators, for which a tertiary treatment step is required to achieve the desired quality of reclaimed water.

While streamlining the focus on disinfection using existing treatments like ozone, UV and membrane filtration, secondary effluent also contains physical and chemical constituents that can hinder pathogen inactivation and drastically reduce treatment effectiveness. While using UV, turbidity, TSS and organics present in wastewater can interfere during treatment making it ineffective and demands frequent maintenance to control the fouling of tubes. Ozonation can be uneconomical for wastewater with a high concentration of solids, organic carbon, BOD and COD (Pulido, 2005). These barriers suggest a pre-treatment step to achieve pre-disinfected wastewater quality to ensure high disinfection efficiency which in turn increase the operational cost of the treatment scheme.

While many different treatment options exist, adequate removal of all pollutants is extremely complex due to their wide diversity. Hence, it is important to evaluate the ability of technology to remove a varied range of contaminants since a combination of approaches will be needed to ensure safe water reuse. EC has become increasingly popular over the years for its ability to remove a wide range of pollutants. Previous studies have shown effective removal of virus, bacteria and protozoa indicators from synthetic groundwaters, surface waters and domestic wastewater using iron and aluminium electrodes (Delaire et al., 2017; Estrada et al., 2017; Boudjema et al., 2014). However, the removal of antibiotic-resistant bacteria in domestic wastewater has not been thoroughly investigated.

Further, studies with EC have shown an effective reduction of contaminants like COD, arsenic, nitrate, organic matter, suspended particles, heavy metals and refractory organic pollutants (Symonds et al., 2014) in industrial wastewater. Treatment of domestic wastewater with aluminium and iron electrodes has shown a great reduction of turbidity by 90%, COD by 75%, phosphorous by 98% and 'complete disinfection' per the absence of faecal coliforms in treated effluents (Symonds et al., 2014; Chen et al., 2000). The iron hydroxide flocs generated during the process are observed to have affinity

with compounds like phosphate and COD. Whereas, when the positively charged coagulants adsorb effluent organic matter, excess adsorption is observed to reverse the surface charge of ferric/aluminium hydroxides from positive to negative inhibiting the removal of negatively charged colloids and microbes (Abudalo et al., (2009).

The application of EC for municipal wastewater treatment signifies a potential alternative due to the ease of operation, simple design and choice to treat other wastewaters; however, the capability of EC as an effective tertiary treatment system to reduce the overall concentration of pollutants has not been reported so far. Previous EC research on domestic wastewater has largely focused on current density (due to its effect on charge dosage) as the main variable controlling pollutant removal. The effect of charge dosage rate on removal or treatment time is not investigated yet, despite its effect on the average contact time between pollutant and Fe(III) precipitates in the solution, in addition to possible effects on the rate of pollutant oxidation, making it critical to understand EC performance and mechanisms (Amrose et al., 2015).

The focus of this research is to assess the capability of low voltage iron EC to reduce the concentration of enteric pathogen indicators and antibiotic-resistant bacteria in municipal wastewater effluent. Additionally, the removal of wastewater quality parameters must be studied as the knowledge of pathogen-organics-electro coagulant interaction is crucial for a precise evaluation of the system.

### **1.3 Research question and objectives**

#### **1.3.1 Research question**

To what extent can low voltage iron EC remove enteric pathogen indicators and antibiotic-resistant bacteria from secondary municipal wastewater effluent? Is co-removal of wastewater parameters such as phosphorous, total nitrogen, COD, TSS, turbidity and colour achieved along with microbial attenuation?

#### **1.3.2 Hypothesis**

EC can achieve effective reduction of pathogen indicators and antibiotic-resistant bacteria in the presence of wastewater quality parameters. The electro-coagulants generated benefit the reduction of phosphorus, COD, solids, total nitrogen present in secondary wastewater effluent.

### 1.3.3 Goals and objectives

The goal of this research is to evaluate EC in lab-scale for the removal of enteric pathogen indicators: *E. coli*, Enterococci, Somatic coliphages and *Clostridium perfringens* spores and antibiotic-resistant bacteria: *ESBL E. coli* and Vancomycin-resistant Enterococci from secondary wastewater effluent.

The specific objectives include:

1. Evaluating the treatment performance in different water matrices: demineralised water, synthetic municipal wastewater effluent and real municipal wastewater effluent.
2. Examining the effect of operational parameters in terms of charge dosage and charge dosage rate.
3. Evaluating the removal of phosphorous, total nitrogen, COD, TSS, turbidity and colour.
4. Verifying the effect of treatment on pathogen removal by modelling removal kinetics

## Chapter-2

# Literature review

### 2.1 Pathogens in municipal wastewater

Municipal wastewater composition creates an ideal environment for a wide range of enteric pathogens such as virus, bacteria, protozoa, parasitic worms and eggs. Testing wastewater samples for the entire range of pathogenic organisms is not feasible due to very costly, labor-intensive procedures and due to the fact that only less than 2% of microbes can be cultured in the laboratory (Wade, 2002). Hence, monitoring microbiological water quality is based on the detection and enumeration of fecal indicator organisms that share similar characteristics with the pathogens (Chahal et al., 2016). The most common pathogens present in wastewater and the infections associated with them are discussed below.

#### 2.1.1 Bacteria

Bacteria form the most diverse group of human pathogens in municipal wastewater. Several types of bacteria inhabit in the human intestine and are shed in feces. Of these populations, many are commensal and useful to their hosts whereas, some are pathogenic which form the majority of bacterial pathogens in wastewater. The major human bacterial pathogens include *Salmonella spp.*, *Escherichia spp.*, *Shigella spp.*, *Vibrio cholera*, *Mycobacterium spp.*, *Legionella pneumophilia* and *Pseudomonas*. The diseases associated with these pathogens include gastroenteritis by *Campylobacter jejuni* and *Escherichia coli*, Salmonellosis, typhoid and paratyphoid by *Salmonella spp.*, Bacillary dysentery by *Shigella spp.*, and cholera by *V. cholerae*.

Fecal coliforms, *E. coli* and intestinal Enterococci are referred to as ‘fecal indicator bacteria’ and their presence may indicate potential fecal contamination in water. The coliform group is composed of Gram-negative rod-shaped bacteria belonging to the family Enterobacteriaceae. *E. coli* is present in high concentration in the feces of warm-blooded animals and has been extensively used as an indicator of fecal contamination in environmental waters. Intestinal Enterococci are gram-positive cocci which are found in feces of warm-blooded animals. They include the species *E. faecalis*, *E faecium*, *E.durans*

and *E. hirae*. Along with *E. coli*, Enterococci is extensively used as an indicator of fecal contamination (Chahal et al., 2016).

The concentrations of fecal indicator bacteria can vary from  $10^4$  to  $10^5$  cfu/100 ml in secondary wastewater effluent. WHO recommends *E. coli* concentration in reclaimed water to be less than 10 cfu/100 ml for use in unrestricted irrigation (WHO, 2018).

### **2.1.2 Viruses**

Municipal wastewater harbours a wide variety of viruses originating from human gastrointestinal tracts and are referred to as enteric viruses. Viruses are small (15-80 nm) infectious particles, with a nucleic acid core (single or double-stranded DNA or RNA) or enclosed in protein coat or capsid. Many outbreaks are associated with enteric viruses because the infectious dose is lower than those associated with bacterial infections. The common viruses causing water-borne diseases include rotaviruses, noroviruses and adenoviruses.

Bacteriophages have been used as model organisms for enteric virus due to their similarities in composition, morphology, structure, size and site of replication. Two groups of bacteriophages, somatic coliphages and F-specific coliphages are used as indicators. They are used due to their abundance in fecally contaminated water, fast, easy, cost-effective detection and enumeration techniques and similar resistance to treatment as that of human pathogenic viruses. F-specific phages are bacteriophages that infect Gram-positive bacteria, including *E. coli*. Somatic coliphages are DNA phages that infect strains of *E. coli* and are potentially capable of multiplying if the specific host bacterium is metabolizing in wastewater (Jofre et al., 2016). Somatic coliphages have been proposed as potential surrogates of enteroviruses due to similar decay rates during treatment, seasonal variation and resistance to environmental factors (Chahal et al., 2016; Dias 2016).

### **2.1.3 Protozoa**

Protozoa form another classification of microorganisms that are found in wastewater. They are either free-living or parasitic in nature. *Cryptosporidium parvum*, *Cryptosporidium hominis* and *Giardia duodenalis* are the common protozoan parasites. *Cryptosporidium* is spread in the form of a non-reproductive and dormant oocyst from feces. They infect the host, causing diarrhoea, nausea and abdominal pain. *Giardia* is also transmitted in a dormant cyst stage and causes an infection called giardiasis, causing acute diarrhoea, nausea, malabsorption, abdominal pain and weight loss. The threat from these protozoa parasites is due to their high resistance to chlorine, low infection dose, persistence in the environment and comparatively expensive and complex detection and measurement of

infectivity. The bacterium *Clostridium perfringens*, a spore-forming anaerobe of 1µm in size is considered a conservative indicator for pathogenic protozoa. They are found abundantly in feces of warm-blooded animals. These spores have been associated with the occurrence of *Cryptosporidium oocysts* and *Giardia cysts* in municipal wastewater (Chahal et al., 2016).

#### **2.1.4 Antibiotic-resistant bacteria**

The existence of antibiotics and resistance against them has occurred in nature well before human interference. Resistant elements have been identified in bacterial DNA which has been isolated for 30,000 years in permafrost (Costa et al., 2011). However, a significant human influence on the excessive use of antibiotics has accelerated the rise of bacterial resistance in areas where antibiotics are used and in aquatic environments. Bacteria have developed various mechanisms to resist the antibiotics used against them. The genes encoding these defense mechanisms are located on bacterial chromosomes or plasmids and are transmitted to the next generations i.e., vertical gene transfer. Also, the genetic elements like plasmids can be exchanged between bacteria of same and different taxonomic affiliation i.e., horizontal gene transfer (Schwartz et al., 2003). Though bacterial resistance has existed long before the antibiotic era, the dangerous resistant strains have taken a disturbing regularity as of the past 20 years.

Among the dangerous gram-positive and gram-negative bacteria, the threats from gram-positive bacteria are widespread and destructive, responsible for most bacteria-related deaths in the United States (Fair and Tor, 2014). In the past ten years, a new wave of gram-negative strains as dangerous as gram-positive strains has emerged. The gram-negative strains are perilous due to their higher prevalence of efflux pumps and non-penetrative outer membranes which make them naturally resistant to few antibiotics (Fair and Tor, 2014). The most common threatful gram-positive strains include vancomycin-resistant Enterococci (VRE), methicillin-resistant *Staphylococcus aureus* (MRSA) and vancomycin-resistant *Staphylococcus aureus* (VRSA). Of the gram-negative strains, carbapenem-resistant Enterobacteriaceae (CRE), multi (MDR) and pan (PDR) drug-resistant *E. coli*, Enterobacter, *Pseudomonas aeruginosa*, *Klebsiella pneumonia* (Fair and Tor, 2014) (Arias and Murray, 2009).

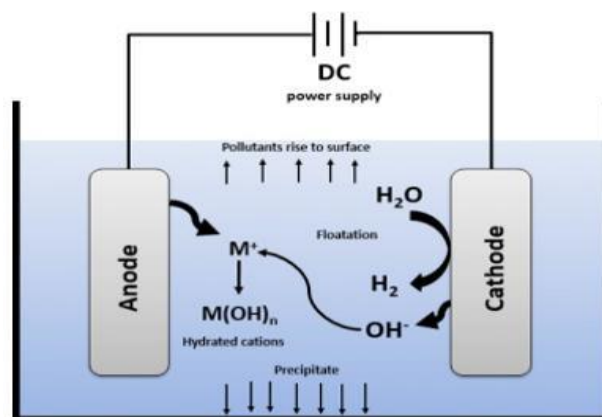
Resistant Enterococci: Enterococci are considered dreadful pathogens due to their resistance to antimicrobial agents. All Enterococci are intrinsically resistant to several anti-microbial agents and thus exhibit low-resistance to penicillin, cephalosporins, carbapenems, and carbacephems. They have also acquired genes to resist other agents including vancomycin. Currently, vancomycin is considered a last resource antibiotic to drug-resistant Enterococci and methicillin-resistant staphylococci. The

largest threat from vancomycin-resistant Enterococci is not from these organisms but their potential to transfer their resistant genes to other more pathogenic gram-positive bacteria (Moellering,1998).

Resistant *E. coli*: *E. coli* is one of the most antibiotic-resistant strains among the Enterobacteriaceae family. Specifically, Extended-Spectrum Beta-Lactamase (ESBL) producing *E. coli* are emerging worldwide. *E. coli* in multiple continents have acquired New Delhi Metallo- $\beta$ -lactamase-1 enzyme from *K. pneumoniae* which provides broad resistance to all  $\beta$ -lactams including carbapenems (Fair and Tor, 2014). ESBL producing strains are feared as they are resistant to all penicillins, cephalosporins (including third and fourth generation agents) and aztreonam. Further, they are usually cross-resistant to trimethoprim/sulfamethoxazole and quinolones. This mix of properties can significantly affect the outcomes of infections both in the community as well as in hospital settings (Picozzi et al., 2014). The risk of highly resistant strains is intensifying due to horizontal gene transfer.

## 2.2 Theory of electrocoagulation

In EC, a potential is applied to the metal electrodes which causes two separate reactions. The chemical reactions- oxidation and reduction occur at the anode and cathode respectively, at the electrode-electrolyte interface. The sacrificial anode releases metal ions and cathode generates hydroxyl ions and hydrogen gas. The ions further hydrolyse to respective hydroxides and form coagulants. Figure 1 shows the electrochemical reactions occurring during electrocoagulation.

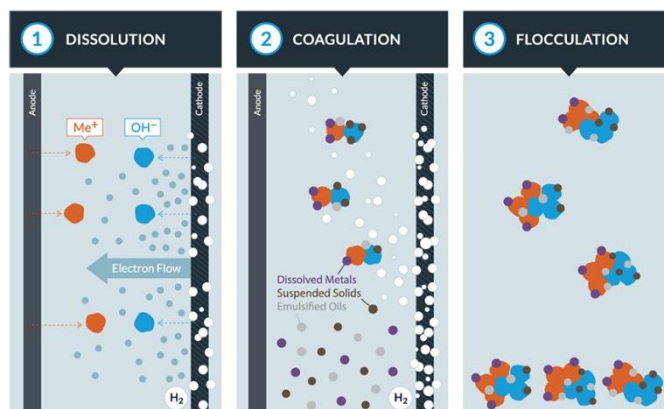


Source: Moussa et al.,2016

Figure 1 Electrochemical process during electrocoagulation

In EC process, the coagulating ions are produced 'in situ' and involves the three stages as shown in Figure 2.

- (i) Formation of coagulants due to electrolytic oxidation of the 'sacrificial electrode'.
- (ii) Destabilization of contaminates and particle suspensions.
- (iii) Aggregation of destabilized phases to form flocs.



Source: Water tectonics.com

Figure 2 Coagulation and flocculation mechanism in electrocoagulation

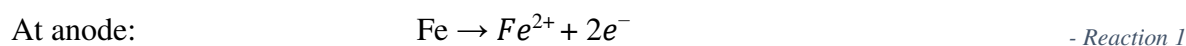
The destabilization mechanism of pollutants can be summarized as compression of the diffuse double layer around the charged species by interaction with ions generated by oxidation of sacrificial anode. Charge neutralisation of ions in wastewater takes place by counter ions produced during electrochemical dissolution, floc formation which creates a sludge blanket and entraps colloidal particles. The solid oxides, hydroxides and oxyhydroxides produced during the process provide active sites for the adsorption of polluting species (Garcia-Segura et al., 2017).

In addition, the following physicochemical reactions occur in an EC cell:

1. Reduction of impurities present in the wastewater at the cathode.
2. Electrophoretic migration of ions in the solution.
3. Electro-floatation of coagulated particles by hydrogen bubbles produced at the cathode.

### 2.2.1 Reaction at electrodes

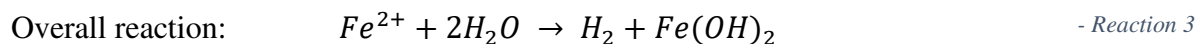
Iron and Aluminium are the most commonly used plate electrodes. The generated iron species undergo spontaneous reactions to form hydroxides and/or poly-hydroxides such as  $\text{Fe}(\text{OH})_3$ ,  $\text{Fe}(\text{OH})^{2+}$ ,  $\text{Fe}(\text{OH})_2^+$ ,  $\text{Fe}(\text{OH})_4^-$ . Besides, these complexes tend to polymerize as  $\text{Fe}_2(\text{OH})_2^{4+}$  and  $\text{Fe}_2(\text{OH})_4^{2+}$ . When Fe anode is used,  $\text{Fe}^{2+}$  is dissolved in the wastewater following iron oxidation as shown in Reaction 1.



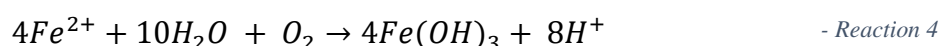
At the cathode, OH<sup>-</sup> and H<sub>2</sub> gas are produced upon reduction as shown in Reaction 2. Production of OH<sup>-</sup> increases the pH during electrolysis leading to the formation of different iron hydroxy complexes.



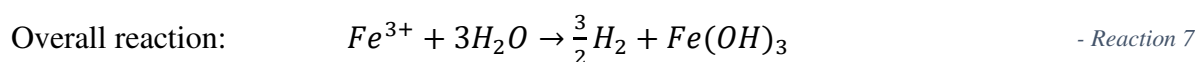
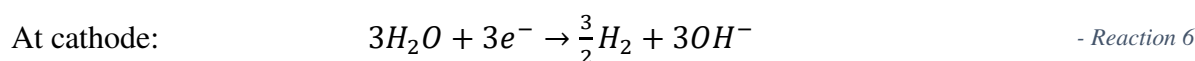
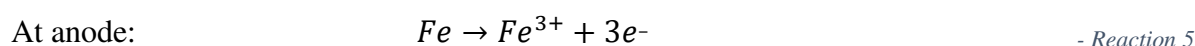
The ferrous ion is hydrolysed to form ferrous hydroxide and hydrogen gas as shown in Reaction 3.



Under the action of dissolved oxygen, Fe<sup>2+</sup> is oxidized to Fe<sup>3+</sup> to form insoluble Fe(OH)<sub>3</sub> as shown in Reaction 4.

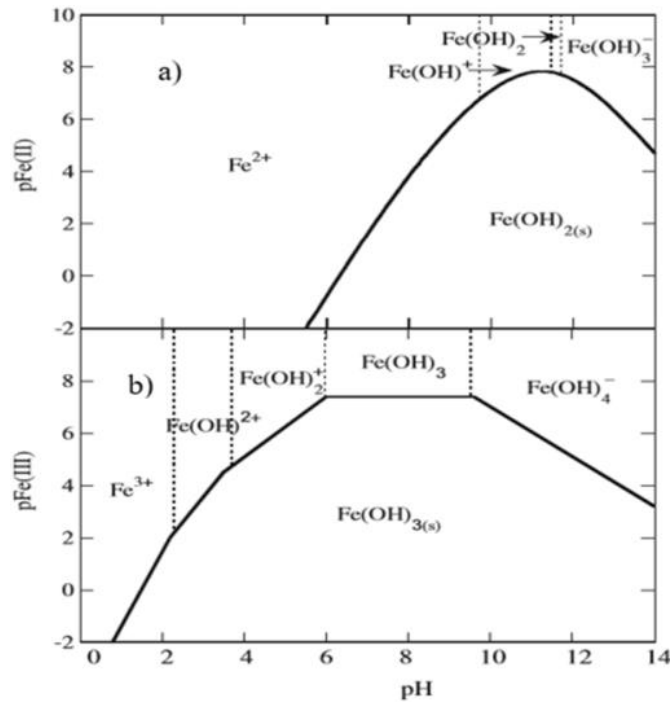


The oxidation of anode generating Fe<sup>3+</sup> ions and its further hydrolyzation to form its respective hydroxides are shown in Reaction 5, 6 and 7.



The Fe<sup>3+</sup> generated may also produce polymeric hydroxy complexes such as Fe(H<sub>2</sub>O)<sub>6</sub><sup>3+</sup>, Fe(H<sub>2</sub>O)<sub>5</sub>(OH)<sup>2+</sup>, Fe(H<sub>2</sub>O)<sub>4</sub>(OH)<sup>2+</sup>, Fe<sub>2</sub>(H<sub>2</sub>O)<sub>8</sub>(OH)<sub>2</sub><sup>4+</sup> and Fe<sub>2</sub>(H<sub>2</sub>O)<sub>6</sub>(OH)<sub>4</sub><sup>4+</sup> based on the pH range of wastewater. The stability of Fe<sup>2+</sup>, Fe<sup>3+</sup> and their hydroxide complexes is influenced by the pH, determined using a predominance zone diagram as shown in Figure 3. Fe(OH)<sub>2</sub> precipitates at a pH higher than 5.5 and remains in equilibrium with other monomeric species such as Fe<sup>2+</sup> until pH 9.5, Fe(OH)<sup>+</sup> from pH 9.5-11.4 and Fe(OH)<sub>3</sub> from 11.8-14 as shown in Figure 3a. Whereas, Fe(OH)<sub>3</sub> precipitates from pH 1 as shown in Figure 3b. The precipitated species stay in equilibrium with other monomeric species at different pH ranges. Fe(OH)<sub>3</sub> stays in equilibrium with Fe<sup>3+</sup> until pH 2, with Fe(OH)<sup>2+</sup> between pH 2-4, with Fe(OH)<sup>2+</sup> between 4-6, Fe(OH)<sub>3</sub> between 6-10. Fe(OH)<sub>3</sub> is the unique species formed between a pH 6-10.

Though Fe<sup>2+</sup> and Fe<sup>3+</sup> form coagulating agents, Fe<sup>3+</sup> outperforms coagulation-flocculation process due to its higher charge density. The process is favoured by the higher charge valence ion which effectively decreases the electric double layer as a high pollutant removal is dependent on the charge valence ion. Of all Fe<sup>3+</sup> species, Fe(OH)<sub>3</sub> is the most preferred coagulant and responsible for pollutant removal (Garcia-Segura et al., 2017).



Source: Garcia-Segura et al., (2017)

Figure 3 Predominance zone diagram of iron as a function of pH

The hydroxides/polyhydroxides compounds formed have a strong affinity for dispersed particles including counter ions to cause coagulation. The gases evolved near the electrodes can cause floatation of the coagulated materials. Since hydrogen and oxygen bubbles are produced at the cathode and anode respectively, the EC process is intrinsically associated with electro-floatation. The produced gas bubbles behave as insulating spheres and can increase the electrical resistance resulting in high electric energy to achieve optimum removal efficiency. Hence, to minimize the accumulation of bubbles at the electrode surfaces, the electrolyte flow must be increased to sweep out the bubbles (Mollah et al., 2004).

### 2.3 Electrocoagulation for wastewater disinfection

The electrochemical generation of coagulants in a pollutant treatment reactor has the feature of precise process controllability, and the extent of coagulant generation can be profitably attuned with the demand imposed by the degree of pollution in wastewater (Pulido, 2005).

EC technology offers many distinctive advantages. The following list summarizes a few of the positive features of the electrochemical approach for pollutant removal.

1. Environmental compatibility – Electron is the main reagent and no need for additional chemicals.

- 2. Versatility
  - Direct or indirect oxidation can produce neutral, positively or negatively charged organic, inorganic or biochemical species.
  - The pollutants can be solid, liquid or gaseous in nature. Also, wastewater volumes can vary from microlitre to millions of litres
- 3. Energy efficiency
  - EC reactors can be designed to control applied voltages and minimize power losses during voltage drops or poor current distribution.
- 4. Safety
  - Utilization of mild conditions and use of harmless nature of coagulants.
  - Direct current is safer than alternating current.
  - The applied potential can be altered to attack selective bonds and avoid the production of by-products.
- 5. Cost-effectiveness
  - The equipment and its operation are normally simple and can be relatively cheap if designed appropriately.
- 6. Reliability
  - Accurate iron dosing using Faraday's law.

Along with these advantages, some challenges like complexation, oxidation of electrode materials, release of gases of explosive nature, high cost of electricity in few locations and lack of understanding of electrochemistry can be the greatest barriers.

Disinfection by electrocoagulation depends on the wastewater parameters such as temperature, pH, nature of electrodes and energy input. Removal of pathogens is either by inactivation or physical attenuation. The inactivation can be directly due to the electric field or due to the generation of active chemical species such as free radicals or ions like  $\text{OH}\cdot$ ,  $[\text{O}]$ ,  $\text{HO}_2\cdot$ ,  $\text{Cl}_2$ ,  $\text{OCl}\cdot$ . The electric field is proven to harm cells by disrupting cell walls. Electro-sorption of bacteria onto the electrode surface and its subsequent destruction aids direct inactivation (Tanneru & Chellam, 2012; Ghernaout et al., 2008). The physical attenuation is mainly by adsorption, sweep coagulation, charge neutralisation by the metal hydroxide flocs produced during the process.

## **2.4 Effect of operational parameters**

### **2.4.1 Electrode material**

Electrode material determines the effectiveness and efficiency of the treatment. The effectiveness depends on anodic dissolution and coagulants needed for effective removal of pollutants. Higher charge of coagulating ion such as  $\text{Fe}^{3+}$  is preferred as they can compress the electric double layer effectively to aid coagulation. Though  $\text{Fe}^{2+}$  behaves as a coagulant,  $\text{Fe}^{3+}$  is preferred due to a higher positive charge and higher solubility of hydroxides. However, Aluminium and Iron are the most preferred electrode materials also due to their easy availability, low cost and high rate of dissolution (Garcia-Segura et al., 2017).

### **2.4.2 Initial pH**

Initial pH of wastewater is a critical operational parameter affecting the electrochemical process. pH during the process varies depending on the initial pH and type of electrode material. pH affects the process firstly, by altering the equilibrium of different species related to coagulant formation. Secondly, physicochemical properties of coagulants are changed such as solubility of metal hydroxides, size of colloidal particles of coagulant complexes and electrical conductivity of metal hydroxides. Thirdly, it can influence different anions or inert species present in the actual water matrix, affecting their charge and influencing double-layer shielding of coagulants or its oxidative nature (Lakshmanan et al., 2009).

Irrespective of the initial value, the pH during EC increases due to the production of  $\text{OH}^-$  ions and stabilizes to initial pH once the current is turned off. Maintaining an alkaline initial pH prevents greater changes in pH and decreases the efficiency of pollutant removal. Whereas, acidic or circumneutral pH have shown higher removal efficiencies (Kobyta et al., 2003).

### **2.4.3 Electrocoagulation time**

Treatment time plays an important role in all the electrochemical treatments as it influences the formation, concentration of metal hydroxides and pollutant removal. EC time is calculated by the ratio of charge dosage to charge dosage rate. Variation in time, based on the charge dosage rate determines the production of coagulant concentrations. Low charge dosage rate allows a longer contact time enabling enough adsorption of pollutants on to the flocs. However, a longer contact time also reduces floc density and their settling velocity (Amrose et al., 2013).

#### 2.4.4 Charge dosage

Charge dosage,  $q$  (C/L) is the total charge passed through the solution by the current. It is related to the active electrode surface area  $A(\text{cm}^2)$ , wastewater volume  $V(\text{m}^3)$ , electrolysis time  $t$  (s) and the current density given by  $J = I / A$  ( $\text{mA}/\text{cm}^2$ ) (Amrose et al.,2013). Charge dosage is determined by the relation as shown in Equation 1.

$$q = \frac{J \times t \times A}{V} \quad \text{- Equation 1}$$

The charge dosage determines the concentration of iron, Fe (mg/L) generated during the process considering a constant operating current (I) and assuming iron to be the only electrochemically active species. It is related to the molecular weight of iron,  $M$  (mg/mol), Faraday's constant,  $F$  (C/mol), number of moles of electrons per mole of iron, ( $n=2$ , assumed) (Amrose et al., 20 13). The relation for calculating the theoretical mass of iron dissolved is given by Faraday's law as shown in Equation 2.

$$Fe_{theo} = \frac{q \times M}{n \times F} \quad \text{- Equation 2}$$

The efficiency of iron production can be determined using Faradic efficiency (FE) and is determined by the ratio of experimental mass of Fe to theoretical mass of Fe as shown in Equation 3. A FE of 1 means an ideal production on the anode as predicted by Faraday's law, i.e., all charge passed through goes to Fe(II) production and transport to the bulk electrolyte. A  $FE < 1$  suggests that Fe production and transport to the bulk is not ideal, resulting in a lower Fe dose. A low Fe dose can originate from two main reasons, i) Fe(0) oxidation is limited or absent due to competing side reactions like oxidation of water or b) Fe(II) is produced but does not end up in the bulk electrolyte.

$$FE = \frac{Fe_{exp}}{Fe_{theo}} \quad \text{- Equation 3}$$

where  $Fe_{exp}$  is the experimental mass and  $Fe_{theo}$  is the theoretical mass of iron dissolved in mg/L.

Previous studies have reported current density to be the key controlling factor determining pollutant removal efficiency (Pouet and Grasmick, 1995), while others observed no significant effect of current density on pollutant removal (Chen et al., 2000). Current density and treatment time used in each study is specific to their respective treatment conditions, in terms of wastewater volume, electrode surface area and water/wastewater quality. If the same removal efficiency as obtained in previous studies must be achieved, then the exact same operating conditions in terms of current density, volume, electrode area, treatment time and wastewater quality must be assured. This criterion poses few challenges while designing EC reactors or during practical applications for larger volumes, as electrode area and

wastewater volume can be rarely maintained constant. Hence, it is necessary to identify the most applicable scaling parameter for the effective performance of EC.

#### 2.4.5 Charge dosage rate

The charge dosage rate (CDR) is the amount of coagulant generated per volume of solution per unit time. The dosage rate  $dq/dt$  (C/L/min) is proportional to the rate of iron dissolution per unit volume of wastewater during the process (Gadgil et al., 2014) (Amrose et al., 2013). The relation is given by Equation 4.

$$\frac{dq}{dt} = \frac{I}{V} = \frac{J \times A}{V} \quad \text{- Equation 4}$$

where I is the operating current (A), V is the volume of water ( $m^3$ ), J is the current density ( $mA/cm^2$ ), A is the area ( $cm^2$ ).

As expressed in section 2.4.3, CDR can be used to calculate the minimum EC time using the desired charge dosage. It also controls the average contact time between ferric hydroxide precipitate and the pollutant present in the wastewater. At a low CDR, the treatment time is less for a low q, while an increment in charge dosage leads to longer treatment time. Whereas, at high CDR, the charge dosage increment can be achieved within a shorter treatment time. In a study conducted by Amrose et al., (2013), EC time and q correlated strongly with dosage rate and not with current density. Application of high CDR with short treatment time can be useful in locations with intermittent power supply (S. Muller et al., 2019). However, a higher rate increases the power consumption due to a higher voltage and total electric work required to transfer the amount of charge. Hence, it is necessary to find the optimum charge dosage rate that provides a high FE and minimizes power consumption (Muller et al., 2017). The equation for calculating the electric power consumption during the process per  $m^3$  of wastewater is shown in Equation 5.

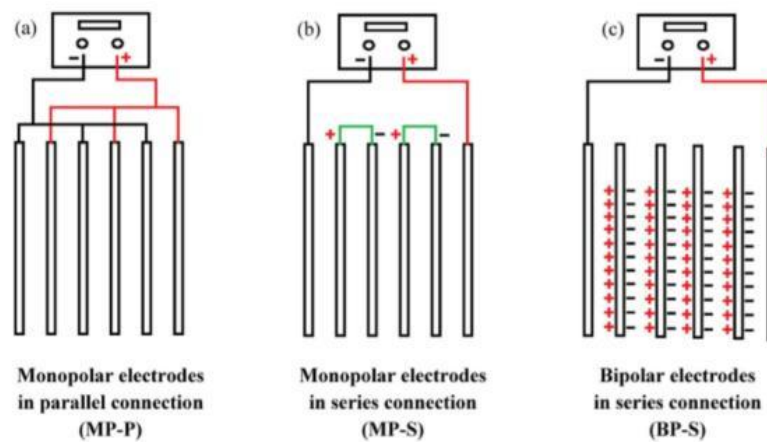
$$P = \frac{E \times I \times t}{V} \quad \text{- Equation 5}$$

where P is the specific power consumption ( $Wh/m^3$ ), E is the cell voltage in volt (V), I is the current in Ampere (A), t is the treatment time in hour (h) and V is the volume of water in cubic meter ( $m^3$ ).

Currently, the effect of charge dosage and charge dosage rate has been applied only in the studies for Arsenic removal (Amrose et al., 2013) (Muller et al., 2017). Similar conclusions from these studies, in terms of treatment parameters are drawn in this study.

## 2.4.6 Electrode arrangements

The connection mode of electrodes determines the pollutant removal efficiency as well as the energy consumption and cost. The most common arrangements are monopolar electrodes in parallel, monopolar electrodes in series and bipolar electrodes in series. The arrangements are shown in Figure 4.



Source: Khaled et al., (2015)

Figure 4 Electrode configurations a) Monopolar in parallel b) Monopolar in series c) Bipolar in series connection

In the monopolar arrangement, each electrode works as anode or cathode based on its electrical polarity in the electrochemical cell. In a parallel connection, each sacrificial anode is directly connected with another anode in the cell, similarly for the cathodes. In serial connection, each pair of anode-cathode is interconnected but are not connected with outer electrodes. Whereas in a bipolar arrangement, each electrode except the ones on the extreme ends (which are monopolar) presents different polarity at each of the electrode sides depending on the charge of the electrode in front of it. The connections are always maintained in serial mode.

Few authors have compared the performances with different electrode arrangements, but the results are not completely conclusive as the relative efficiencies depend strongly on wastewater quality and operational parameters discussed in the previous sections. However, previous studies report monopolar electrode in parallel connection to have low operational costs and favour higher pollutant removal due to low electrode gap. A higher gap increases resistance to mass transfer which leads to high energy consumption. While bipolar arrangement requires lower installation maintenance (Garcia-Segura et al., 2017) (Khaled et al., 2015).

#### **2.4.7 Inter-electrode distance**

Inter-electrode distance is an important parameter in optimizing operational costs of the system. An increase in the distance increases the ohmic loss with respect to anode-cathode and resistance to mass transfer. Khaled et al., (2015) reported slowing down of kinetics of both charge transfer and anode oxidation at a larger inter-electrode gap, which resulted in a lower pollutant removal efficiency. Abbas and Ali, (2018) reported that inter-electrode distance can be varied depending on the conductivity of wastewater. The optimum range is between 0.5-2cm. Though a higher electrode-distance can reduce the capital cost of treatment, the treatment efficiency is reduced.

#### **2.4.8 Surface area to volume ratio**

The ratio of the active surface area of the electrode to treated volume is an important design parameter in EC. Previous studies reported a higher S/V ratio to reduce the current density used during the experiments (Khaled et al., 2015). A higher S/V ratio promotes electrical transport, better chemical dissolution of metal anode, better pollutant removal efficiency and reduces costs. Hence, this parameter is crucial when aiming for an efficient process.

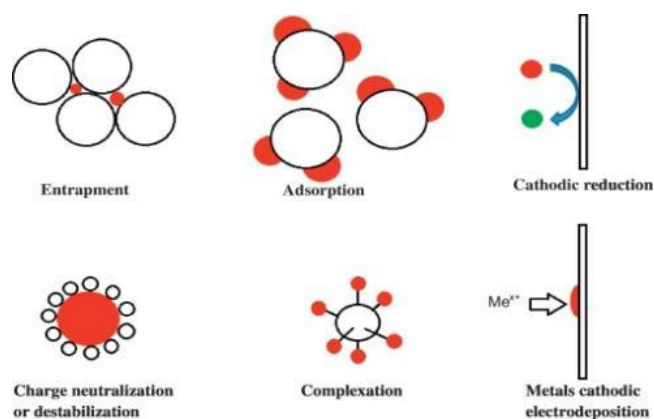
#### **2.4.9 Stirring speed**

The main function of stirring speed is to efficiently transfer coagulants produced at the electrodes throughout the wastewater. It is crucial as it causes homogenization of system variables such as pH, temperature. Low stirring speed can cause inhomogeneity of wastewater and very high speed can destroy flocs resulting in smaller flocs which are difficult to settle. Bayar et al., 2011 reported an optimal stirring rate of 150 rpm to achieve the highest COD removal efficiency in municipal wastewater.

### **2.5 Pollutant removal mechanisms**

The pollutant removal mechanisms are based on the charge, size, hydrophobicity of pollutant and dosage of coagulant. In a wastewater matrix, the stoichiometric reactions lead to charge neutralization, where the cationic metal hydrolysis species neutralize negatively charged particles. In addition, the charge shielding ability of coagulants compress the double layer around the pollutant and thus favour formation of aggregates and subsequent precipitation. Overgeneration of electro-coagulants past solubility levels result in insoluble amorphous metal hydroxides precipitates which entraps pollutants by sweep flocs. Coagulants adsorb or trap ions, organics, microorganisms in wastewater. The negative charge carried by bacteria, viruses and protozoa is prominently removed by adsorption, destabilization and sweep floc mechanisms (Li et al., 2017). Gram-negative bacteria such as *E. coli* carry negative

charge due to phospholipids and lipopolysaccharides in their outer covering. The negative charge on *Cryptosporidium oocysts* is believed to rise from carboxylic acid groups in surface proteins (Searcy et al., 2006). Viruses being DNA or RNA units contain a protein coat carrying a negative charge due to the carboxyl groups which react with metal coagulant species enabling destabilization. Figure 5 shows the most important pollutant removal mechanisms in EC process.



Source: Garcia-Segura et al., (2017)

Figure 5 Important pollutant removal mechanisms during electrocoagulation

In addition to these mechanisms, microbial inactivation by direct killing of cells at high current intensity  $>1$  A has been observed in previous studies (Estrada et al., 2017; Grasmick et al., 2006). Li et al., (2004) and Ghernaout et al., (2008) reported the requirement of oxidants such as  $\text{HO}^\cdot$ ,  $\text{O}_3$ ,  $\text{H}_2\text{O}_2$  to provide additional microbial reductions as a result of cell membrane damage. Delaire et al., (2016) reported that microbial attenuation can also take place by inactivation due to the reactive species such as Fenton reagents released during upon Fe(II) oxidation by  $\text{O}_2$ .

## 2.5.1 Microorganisms

### 2.5.1.1 Bacteria

C. Delaire et al., (2016) observed the removal of Gram-positive strain, *Enterococcus faecalis* in synthetic groundwater by bacteria-ferric hydroxide precipitate adhesion. The phosphate functional group present on the bacterial cell walls rendered negative charge resulting in a strong affinity with ferric hydroxide flocs formed during the process. Estrada et al., (2017) evaluated the removal of *E. coli* in primary and secondary effluents of municipal wastewater using Fe electrodes. Higher log removal in primary effluent than in secondary effluent was observed due to a higher concentration of organic matter which entrapped bacteria upon its adsorption onto the flocs. At a charge dosage  $>480$  C/L and CDR of 12 C/L/min, the removal of 4.62 log units for primary effluent and 3.84 for secondary effluent were achieved. Sruthi et al., (2018) observed a removal of 3.95 log units in tap water spiked

with *E. coli* and 2.53 log units in secondary treated sewage at a charge dosage of 135 C/L and charge dosage rate of 4.5 C/L/min with aluminium electrodes. Ricordel et al.,(2013) reported abatement of *E. coli* due to concomitant processes such as mortality due to depletion of oxygen, adsorption on aluminium flocs and sedimentation.

#### **2.5.1.2 Viruses**

In the study by Zhu et al., 2005, the mechanism of MS2 virus removal by iron coagulation was attributed to adsorption of negatively charged virus particles on to positively charged iron oxyhydroxide flocs. They observed clarification technology to be not crucial for virus removal once they are adsorbed onto the flocs. Estrada et al., (2017) used a very high charge dosage of 480 C/L and CDR of 12 C/L/min and observed Somatic coliphages to be below the detection limit in both primary and secondary municipal wastewater effluent.

#### **2.5.1.3 Protozoa**

Estrada et al., (2017) reported poor decay of *C. perfringens* spores as low as 0.8 and 0.6 log units in both primary and secondary municipal wastewater effluents at a charge dosage >480 C/L and CDR of 12 C/L/min. Bustamante et al., (2001) observed the interaction of spores with both ferric hydroxide flocs as well as hydroxylated aluminium species during coagulation of wastewater. They observed hydroxylated species to electrostatically adsorb on to the negatively charged spores as well as chemisorb due to the specific interaction between both carboxylate and phosphate surface groups present on their surface. The negatively charged carboxylic and phosphate sites functioned as anchoring points where hydrolyzed species would specifically attach and form flocs. Symonds et al., 2014, reported > 4 log removal units of *Bacillus subtilis* spores, which is a surrogate of protozoan parasite *Cryptosporidium* in municipal wastewater. The treatment system functioned in a continuous mode operation at charge dosage >500 C/L and CDR of 15 C/L/min using aluminium electrodes.

#### **2.5.1.4 Antibiotic-Resistant Bacteria**

Delaire et al., (2016) tested attenuation of one gram-positive strain and two gram-negative strains: *Enterococcus faecalis*, *Escherichia coli* K12 (kanamycin-resistant) and *Escherichia coli* ECOR 10 (ampicillin-resistant) in synthetic groundwater using Fe electrodes. At a charge dosage of 66 C/L and CDR of 6 C/L/min, the observed log removal units were 1.5 for both *E. coli* K12 and *E. coli* ECOR 10. A slightly higher removal of 1.9 log units was observed for *E. faecalis*. A similar removal irrespective of their considerably different cell wall structures was due to the phosphate functional

groups on bacterial cell walls which led to bacteria-precipitate adhesion. The phosphate functional group formed the primary binding site for EC precipitates.

## **2.5.2 Wastewater quality parameters**

### **2.5.2.1 Total Nitrogen**

Total nitrogen is the sum of nitrate-nitrogen ( $\text{NO}_3\text{-N}$ ), nitrite-nitrogen ( $\text{NO}_2\text{-N}$ ) and Total Kjeldahl nitrogen (TKN). TKN is the sum of ammonia nitrogen and organic nitrogen. EC is observed to remove partial organic nitrogen but not very effective in the removal of inorganic nitrogen due to weak affinity towards electrogenerated coagulants (Aoudj et al., 2017).

Li et al., (2010) evaluated electrocoagulation for nitrogen-rich wastewater. They observed nitrate to be electrochemically reduced at the cathode to nitrite, ammonia and nitrogen gas and the reduction rate increased with increasing current from 0 to 5A. This was followed by a decrease in nitrate-N concentration and an increase in ammonia-N concentration with time. Nitrite being the intermediate product was produced in very low concentration and further reduced to nitrogen gas or ammonia or oxidized back to nitrate at the anode.

### **2.5.2.2 Phosphorous**

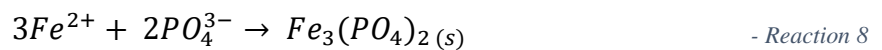
Chen et al., (2000) and Omwene et al., (2018) conducted EC studies on phosphorus removal from municipal wastewater. They reported the removal to be either due to adsorption or co-precipitation based on the initial pH. Amorphous  $\text{Fe}(\text{OH})_3(\text{s})$  "sweep flocs" formed during EC have large surface areas which are useful in the adsorption of phosphate as they have a strong affinity for  $\text{Fe}^{3+}$  ion. Fe oxides in aqueous medium contain surface OH groups, thus phosphate ions undergo ligand exchange with  $\text{OH}^-$ . Adsorption of phosphate on iron oxides leads to inner surface complexation and when water molecules lie between oxide surface and phosphate ion, it results in an outer surface complexation.

Two main mechanisms associated with coagulation of  $\text{PO}_4^{3-}$  with Fe(III) salts include:

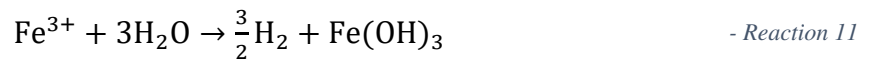
- (i) Formation of  $\text{Fe-OH-PO}_4^{3-}$  complexes. The complexes either adsorb onto Fe(III) hydrolysis species or function as precipitation hubs for Fe(III) hydrolysis products.
- (ii) Direct adsorption of  $\text{PO}_4^{3-}$  ions onto Fe(III) hydrolysis species. Depending on the pH of wastewater, the hydroxides are partially transformed into hydroxyl-complexes (Omwene et al.,2018) (Nguyen et al.,2016).

Phosphorous removal can be directly linked to operational parameters such as initial pH, applied current and electrolysis time, i.e., the charge dosage and dosage rate. Nguyen et al., 2016 observed high P removal in municipal wastewater effluent at an initial pH of 6.5-7. The percentage removal efficiency varied between 94-99.99% at charge dosages of 200-800 C/L and CDR of 100 C/L/min.

Removal was observed to increase with increasing treatment time but decrease with increasing initial pH. However, the type of precipitates formed were varied at different pH ranges (Omwene et al., 2018). At low EC times and  $\text{pH} \leq 6.5$ , Fe-phosphate or hydroxyl-hydroxy phosphate were formed as summarized in Reactions 8, 9 and 10.



At  $\text{pH} \geq 6.5$ , Fe hydroxides were formed as summarized in Reaction 11.



### 2.5.2.3 COD

COD in municipal wastewater is comprised of biodegradable organic compounds, non-biodegradable compounds and inorganic oxidizable compounds. Al-Shannag et al., (2013) reported removal efficiency to be determined by the ability of compounds to react with Fe(II) and Fe(III) to form insoluble compounds. In such cases, the insoluble compounds were completely removed. The share of COD which was not removed comprised of soluble and miscible compounds such as glucose, lactose, phenol, sucrose which do not react with Fe(II)/Fe(III) precipitates to form insoluble compounds. However, a small amount was adsorbed on to the flocs and removed incidentally. High COD removal was attributed to the number of metal ions generated based on the charge dosage.

Ni'am et al., (2014) reported a COD removal of 60 % from synthetic dairy wastewater at 960 C/L and 24 C/L/min after a settling time of 40 min. On increasing the settling time to 240 min, the removal increased to 75% and was enhanced by the settling velocity of suspended particles. They also reported a strong relationship between treatment time (charge dosage) and pollutant removal.

### 2.5.2.4 Total Suspended Solids

In the studies by Bukhari (2008), TSS removal in municipal wastewater was observed to be directly proportional to the applied current and the contact time which is a representative of the charge dosage.

He observed the highest removal efficiency of 92.5% at charge dosage of 300 C/L and CDR of 10 C/L/min. Different TSS removal mechanisms were observed for both ferrous and ferric states. For the soluble ferrous state, the dominant mechanism was charge neutralization, where the removal increased with increasing coagulant dosage, remaining consistent with charge neutralization. Oxidation of soluble ferrous to insoluble ferric state at higher potential (current) resulted in removal through sweep coagulation (Muruganathan et al., 2004) (Bukhari et al., 1999).

Zaleschi et al., (2012) and Hong et al., (2014) observed an increase in suspended solids concentration due to metallic species, hydroxides, carbonates generated in the process, thus indicating a final filtration step to guarantee the quality indicator of treated water.

#### **2.5.2.5 Turbidity**

Turbidity removal in municipal wastewater was observed to be dependent on charge dosage, in the same manner as TSS. Bukhari (2008) observed turbidity reduction from 50 to 14.3 NTU at charge dosage of 300 C/L and CDR of 10 C/L/min. On increasing charge dosage to 500 C/L, the concentration reduced to 3.4 NTU. In the study by Jekel, (1986) and Bukhari, (2008) using chemical coagulation, turbidity increased after treatment. This was observed due to excess current or coagulant dosage, which resulted in restabilization of colloidal particles. Restabilization of colloids occurred due to charge reversal at coagulant doses higher than the optimum value.

## Chapter-3

# Materials and Methods

### 3.1 Experimental setup

The setup was designed to conduct experiments in two 1 L glass beakers simultaneously as shown in Figure 6. The beakers were placed on LABNICO L23 magnetic stirrers and PTFE coated bars were used for stirring. Steel S235 plates (maximum percentages: 0.14% Carbon, 0.10% Silicium, 0.80 % Manganese, 0.025 % phosphorous, 0.015 % Sulphur, 0.010 % Nitrogen, 0.20% Copper and 0.080 % Aluminium) of dimension 6 cm x 4 cm as shown in Figure 7 were used as electrodes. TENMA 72-10500 bench DC power supply of 30 V and 3 A was used as the power source.



Figure 6 Experimental setup for batch-scale experiments



Figure 7 Iron plates used as electrodes for electrocoagulation

### 3.2 Wastewater composition

Electrocoagulation experiments were conducted in three phases. In the first phase, 500 ml demineralised water was spiked with *WRI E. coli* or  $\phi$ X174 Somatic coliphages. Both *WRI E. coli* and  $\phi$ X174 Somatic coliphages cultures were concentrated solutions with the same initial concentration of  $10^7$ - $10^8$  (cfu/pfu)/ml. 1ml of each culture was spiked in 1L of demineralized water to obtain an initial concentration of  $10^5$ - $10^6$  (cfu/pfu)/ml of wastewater. The initial concentration of microbes used in this study was at least 3 logs higher than the concentration in real municipal wastewater effluent collected from a treatment plant in the Netherlands.

In the second phase, a synthetic municipal wastewater effluent was prepared similar to the composition used by Uslu et al., 2016 as shown in Table 1. The organic sources used by Uslu et al., 2006: Yeast extract and peptone were replaced with starch and microcrystalline cellulose in our study to avoid faster degradation of organic compounds (to better represent the left-over COD after AS treatment is degraded slowly or is non-biodegradable). The concentrations of starch, microcrystalline cellulose, urea and dipotassium phosphate were adjusted accordingly to match COD, phosphorous and nitrogen values of the real wastewater effluent used. Investigations in phase-2 were divided into two experiments as described below.

Table 1 Composition of synthetic wastewater effluent

Composition	Concentration (mg/L) (Uslu et al., 2016)	Concentration (mg/L) (Current study)	
		Experiment-1	Experiment-2
Starch / Yeast extract (Uslu et al., 2016)	22	8	8
Microcrystalline cellulose / peptone (Uslu et al., 2016)	32	5	5
Urea	6	8.6	4.3
Dipotassium phosphate	28	5.4	2.7
Sodium chloride	7	60	60
Calcium chloride dihydrate	4	4	4
Magnesium sulphate heptahydrate	2	2	2

In experiment-1, the composition resulted in a COD, phosphorous and nitrogen concentrations of 40-50 mg/L, 0.97 mgP/L and 4.2 mgN/L respectively. In experiment-2, the composition was varied by halving the concentration of phosphorous and nitrogen sources resulting in a final concentration of 0.48 mgP/L and 2.1 mgN/L respectively. Synthetic municipal wastewater effluents were used in both the phases to minimize variabilities in wastewater between treatments and to avoid the complexity of wastewater parameters.

In the final phase, real wastewater effluent from a large municipal wastewater treatment plant (with activated sludge process and no disinfection) in the Netherlands was used. Samples were collected on four different days. The physicochemical characteristics of the effluent are shown in Table 2.

Table 2 Characteristics of real wastewater effluent from a Dutch municipal wastewater treatment plant

Sample no	Date	COD (mg/L)	TSS (mg/L)	Turbidity (NTU)	P (mg/L)	NO <sub>3</sub> <sup>-</sup> (mg/L)	NO <sub>2</sub> <sup>-</sup> (mg/L)	NH <sub>4</sub> <sup>+</sup> (mg/L)	Conductivity (µS/cm)	pH	Cl <sup>-</sup> (mg/L)	True Colour (Pt/Co)
1	13/05/2019	44.40	4.00	1.70	0.40	6.75	1.23	1.08	940	7.25	111.10	55.00
2	15/05/2019	40.10	1.00	1.06	0.23	8.11	0.96	1.37	945	7.30	109.62	53.88
3	20/05/2019	53.40	3.00	1.15	0.49	5.68	0.90	1.18	964	7.27	115.73	85.44
4	22/05/2019	71.40	6.00	1.21	0.39	5.19	0.99	1.42	970	7.28	117.58	85.44

### 3.3 Preparation of microbiological cultures

Electrocoagulation experiments were conducted in three phases to study the removal of microbial indicators in three different water matrices. In the first and second phase, the removal of lab-based, microbial indicators, namely; *E. coli* WR1 strain (NCTC 13167) and φX174 Somatic coliphage (ATCC 1370 6-B1) was studied by spiking them in the wastewater. Due to biosafety considerations, sewage available strains such as *E. coli*, *ESBL E. coli*, VRE, Enterococci, *C. perfringens* spores were not cultured in the available BSL 1 facility. The microbial cultures used in the experiments were prepared as per ISO 10705-2:2000 for Somatic coliphages and ISO 9308-1:2014 for *E. coli*.

#### 3.3.1 Preparation of WR1 *E. coli* Stock culture

A WR1 *E. coli* reference culture vial was thawed from the freezer maintained at -80° C. 0.1 ml from the vial was plated on a few M-Lauryl Sulphate agar plates and incubated at a temperature of 35 ± 3° C for 20 ± 4 h. A culture flask was prepared by adding 50 ml of TYGB and 500 µl of Ca-Glucose into a sterile Nephelometric conical flask. From the incubated plates, a loop-full of 3-5 yellow color

colonies were suspended into the culture flask and incubated at  $37 \pm 1^\circ \text{C}$  for 18h while constantly shaking at a speed of  $100 \pm 10 \text{ rpm}$ . Upon incubation, 10 ml of sterile glycerol was added into the flask and mixed well. Finally, aliquots of 1-1.5 ml were transferred into 2.5 ml cryo-vials and frozen at  $-80^\circ \text{C}$ .

The concentration of the prepared stock culture was tested by preparing serial dilutions ( $10^{-5}$ - $10^{-6}$ ) using phosphate buffer saline. 100  $\mu\text{l}$  of the diluted sample was inoculated on Chromocult coliform agar plates and spread evenly using a sterile spreader. All the tests were carried out in duplicates. The plates were incubated in an invert position at  $36 \pm 2^\circ \text{C}$  for  $21 \pm 3$  hours. The attained concentration was  $5 \times 10^8 \text{ CFU/ml}$ .

### **3.3.2 Preparation of stock cultures of somatic coliphage bacterial host *E. coli* WG5 (ATCC 700078)**

A lyophilized ampoule of reference host culture was rehydrated using approximately 3ml of Modified Scholtens' Broth (MSB). The culture was transferred into a 300 ml conical flask with  $50 \pm 5 \text{ ml}$  of MSB and incubated for  $20 \pm 4 \text{ h}$  at  $36 \pm 2^\circ \text{C}$  on a shaker. 10 ml of sterile glycerol was added in the culture flask and aliquots of 0.5ml were distributed in cryo-vials and stored at  $-80^\circ \text{C}$ .

### **3.3.3 Preparation of working cultures of somatic coliphage bacterial host *E. coli* WG5 (ATCC 700078)**

A stock culture of *E. coli* WG5 was streaked on M-Lauryl Sulphate agar plates and incubated at  $36 \pm 2^\circ \text{C}$  for  $20 \pm 4 \text{ h}$ . A loopful of 3-5 colonies from the agar plates were inoculated into a conical flask with 50 ml of MSB (prewarmed to  $37^\circ \text{C}$ ) and incubated at  $36 \pm 2^\circ \text{C}$  for  $5 \pm 1 \text{ h}$  on a shaker. 10 ml of sterile glycerol was added into the flask and gently mixed. Lastly, aliquots of 1.2ml were distributed in cryo-vials and stored at  $-80^\circ \text{C}$ .

### **3.3.4 Calibration curve of somatic coliphage bacterial host *E. coli* WG5 (ATCC 700078)**

Before starting the calibration, spectrophotometer reading was adjusted to zero using 50 ml of pre-warmed MSB in a nephelometric flask. 0.5ml of the working culture of host *E. coli* WG5 was introduced in the flask and incubated at  $36 \pm 2^\circ \text{C}$  with gentle shaking. The absorbance was measured every 30 minutes and an aliquot of 1 ml was collected for plate counting meanwhile, the flask was placed back in the incubator. 0.1 ml of diluted aliquot was plated on Modified Scholten's Agar (MSA) in duplicates and incubated at  $36 \pm 2^\circ \text{C}$  for  $20 \pm 4 \text{ h}$ . This step was repeated for a duration of 3.5 h. On determining the absorbance and its associated bacterial concentration, a plot of concentration-vs-

absorbance was plotted which provided an approximation of the concentration of host organisms in the MSB without plating. The calibration curve is shown in Figure 8.

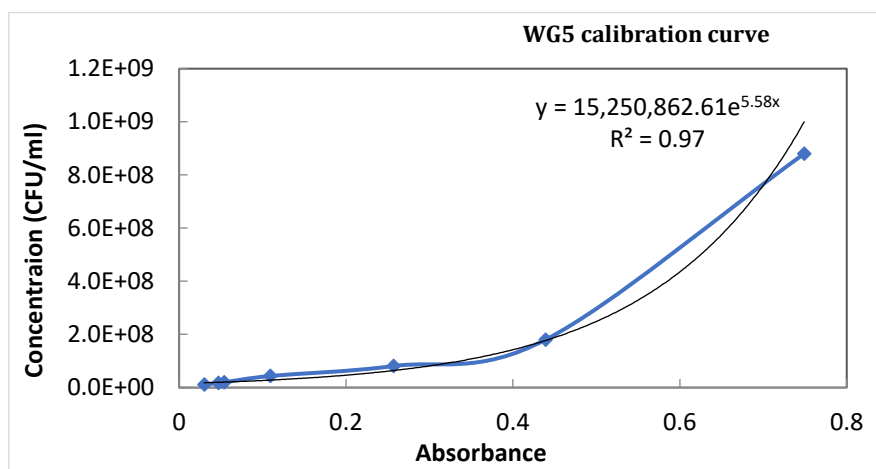


Figure 8 Calibration curve of Somatic coliphages host *E.coli* WG5 (ATCC 700078)

### 3.3.5 Preparation of Coliphage $\phi$ X174 stock

Stock culture of  $\phi$ X174 was procured in high concentration from the Applied Sciences department in TU Delft. The determined concentration of the concentrated stock was  $10^{12}$  pfu/ml. This stock was further diluted with sodium chloride-magnesium sulphate buffer to obtain an initial concentration of  $10^8$  pfu/ml.

## 3.4 Procedure for microbiological assays

### 3.4.1 Bacterial assays

The assays were carried out either by spread plate technique or filtration depending on their concentration. In case of the spread plate technique, 0.1 ml of serially diluted/undiluted wastewater sample was inoculated on specific agar plates and spread using a sterile spreader. In the case of filtration, the wastewater sample was vacuum filtered using 0.45-micron cellulose acetate filter for bacterial assays and cellulose-nitrate filters for *C. perfringens* spores assay. The filter was placed on the agar plate and incubated. The water/wastewater samples were inoculated in pathogen-specific culture mediums and incubating conditions as shown in Table 3.

Table 3 Specific culture mediums and incubating conditions for different pathogen indicators

Microorganism	Culture media	Incubation conditions	Identification
<i>E. coli</i>	Chromocult	21 ± 2 h	Violet colonies
	Coliform agar	36 ± 2° C	
<i>ESBL E. coli</i>	Biomerieux	18 - 24 h	Pink/purple colonies
	Chromid ESBL	35 - 37° C	
<b>Enterococci</b>	Slanetz-Bartley	40 - 48 h	Red, maroon/pink colonies
		34 - 38° C	
<b>VRE</b>	Biomerieux	40 - 48 h	Blue-green colonies: <i>E. faecalis</i>
	Chromid VRE	34 - 38° C	Violet colonies: <i>E. faecium</i>
<b>Somatic coliphages</b>	Modified Scholten Agar	21 ± 3 h	Colorless
		36 ± 2° C	
<i>Clostridium perfringens</i> spores	CHROMagar	18 - 24 h at	Orange colonies
	C.perfringens base	35 - 37° C	

### 3.4.2 Somatic coliphage assay

#### 3.4.2.1 Preparation of host (WG5 culture)

*E. coli* WG5 working culture was inoculated into MSB in a nephelometric conical flask and incubated at 36 ± 2° C with gentle shaking in an incubator. The spectrophotometer reading was adjusted to zero using MSB in another conical flask. The absorbance of the inoculum culture was measured every 30 min until the value reached an absorbance of 0.5-0.6 corresponding to a cell density of approximately 10<sup>8</sup> cfu/ml as per the calibration curve in Figure 8. At this point, the culture was taken out from the incubator and quickly cooled by placing it in melting ice. The inoculum culture was used within the same working day.

#### 3.4.2.2 Assay

For the phage assay, 50 ml of semi-solid Modified Scholtens' Agar was melted in boiling water and placed in a water bath at 45 ± 1° C. Upon cooling, 300 µl of a calcium chloride solution and 400 µl of nalidixic acid were added to the semi-solid Modified Scholtens' Agar and mixed well. 2.5 ml of aliquots were distributed into the culture tubes with caps, placed in a water bath at 45 ± 1° C. To the culture tubes, 1 ml of wastewater sample (diluted/undiluted) and 1 ml of inoculum culture (*E. coli*

WG5) were added and mixed carefully avoiding the formation of air bubbles. The content of the culture tube was poured and distributed evenly on a layer of complete MSA in a 9 cm Petri dish. The plates were dried and incubated upside-down at  $36 \pm 2^\circ\text{C}$  for  $(18 \pm 2)$  h. The number of plaques on each plate were counted within 4 h after incubation using indirect oblique light. Each aliquot was examined at least in duplicate.

### 3.4.3 *Clostridium perfringens* spore assay

The assay was performed as per the procedure described in ISO 14189 (2013) with certain modifications such as using CHROMagar *C. perfringens* base instead of Tryptose-Sulfite-Cycloserine Agar. The assays were always carried out by filtering wastewater samples. Before analysis, the water sample was subjected to heat shock treatment at  $70^\circ\text{C}$  for 15 min to kill vegetative cells. The heat-treated sample was then filtered using a  $0.45\mu\text{m}$  cellulose-nitrate membrane filter. The filter was then placed on a freshly prepared CHROMagar plate and incubated at  $38^\circ\text{C}$  for 24 h in an anaerobic environment.

The identification of pathogen indicators: *E.coli*, Somatic coliphages, *Clostridium perfringens* spores, ESBL *E.coli*, Enterococci and VRE on specific culture mediums is shown in Figure 9.

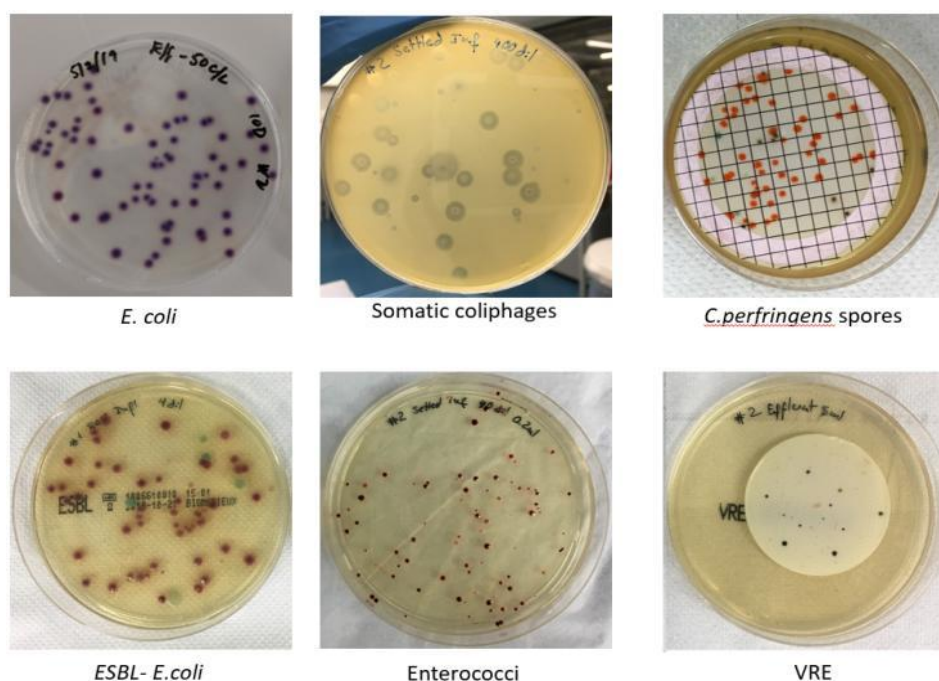


Figure 9 Identification of different pathogen indicators

### 3.5 Physical and chemical analysis

The wastewater pH was measured using WTW ProfiLine 3110 pH meter and the electrical conductance was determined with WTW ProfiLine 3310 portable conductivity meter. Analysis of ions such as  $\text{NO}_2^-$ ,  $\text{NO}_3^{2-}$ ,  $\text{NH}_4^+$ ,  $\text{PO}_4^{3-}$  and  $\text{Cl}^-$  in filtered water samples was carried out with Metrohm 881 basic IC plus and 883 compact IC pro Ion chromatography. Total suspended solids analysis of samples was carried out according to Standard Methods for the Examination of Water and Wastewater 20th Edition (AWWA, 1998). Chemical oxygen demand (COD) analysis was done using HACH test kits in a HACH direct reading DR 3900 spectrophotometer. Turbidity was measured using Turb 430 IR multimeter. Color was analyzed in both unfiltered and filtered samples using UV-VIS spectrophotometer at a wavelength of 410 nm. For the analysis of total nitrogen, Merck cell tests were used. XRD analysis of EC sludge was carried out with Bruker D8 advanced diffractometer operating with Cu K $\alpha$  radiation source. The sludge samples were dried, ground to a fine powder and were filtered with 400 mesh sieves before the analysis. The XRD scans were recorded from  $8^\circ - 110^\circ 2\theta$  with  $0.021^\circ$  step-width and 1s counting time for every step. Iron concentration in the samples was determined using Plasma Quant MS Inductively coupled plasma mass spectrometry (ICP-MS).

### 3.6 Electrocoagulation experiments

The batch experiments in phase 1 and 2 were performed with different synthetic water matrices with a volume of 500 ml. While in phase 3, real secondary effluent was used with a volume of 1000 ml considering the wide range of analyses and the impossibility to adjust the concentration of microbial indicators at will. The conductivity of demi-water in phase 1 was enhanced by adding sodium chloride to reach a range of 900-1000  $\mu\text{S}/\text{cm}$  to match the conductivity of a real secondary effluent. Initial pH in phase 1 and phase 2 was adjusted between 7-7.5 with 0.1 M NaOH/HCl.

EC cell consisted of two parallelly connected plates with an inter-electrode gap of 1 cm. They were electrically connected to a DC power supply and the polarity of electrodes were reversed for each experiment. The electrodes were immersed in wastewater to obtain submerged anode surface area of  $32\text{ cm}^2$  (4 cm x 4 cm) for phase 1 and 2 and  $40\text{ cm}^2$  (5 cm x 4 cm) for phase 3.

#### 3.6.1 Experimental procedure

Experiments were conducted open to the atmosphere at room temperature. Glassware was rinsed thoroughly with demi water and autoclaved prior to use. Before each run, the electrodes were cleaned with fine-grain sandpaper to remove any rust or solid deposits. Wastewater in the glass beaker was stirred continuously with PTFE coated stir bar at a speed of 150 – 200 rpm. Meanwhile, the pH and

conductivity were noted down. To start the experiment, the power supply was adjusted to the required current setting and switched on. Cell voltage was noted down during the start and end of the run. On reaching the actual treatment time, the current source was switched off and electrodes were removed to store them in a container open to the atmosphere at room temperature. pH was measured after switching off the current and the treated water was transferred to an Imhoff cone where it was left to settle overnight.

During the experiment, three sets of samples were collected. First is the influent, before EC. Second is the bulk sample right after the EC treatment and third is the supernatant after overnight settling. The bulk sample was used only for analysis of iron dissolution and the remaining microbial, physical and chemical analysis were done with the supernatant. Figure 10 a, b and c show the three sets of samples: influent, bulk and supernatant respectively collected during the experiment.

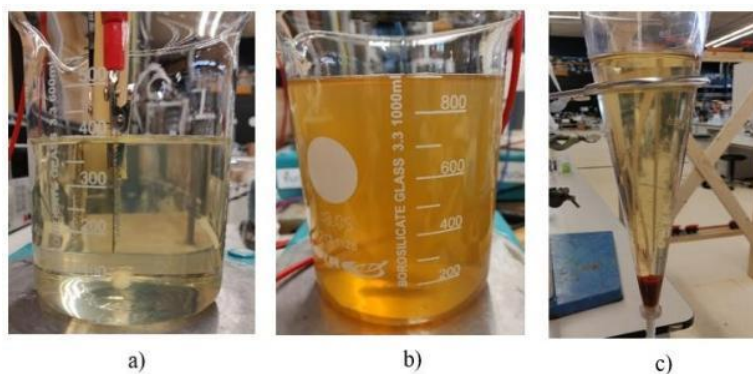


Figure 10 Three sets of samples collected during the experiment a) Influent b) Bulk c) Supernatant

### 3.6.2 Summary of experimental conditions

Several key electrochemical and solution parameters such as charge dosage, charge dosage rate and wastewater compositions were varied in separate experiments to assess their role on microbial attenuation. In this section, the difference between experiments and the major variables used have been summarized.

In phase 1, demi water spiked with *WR1 E.coli* and  $\phi$ X174 Somatic coliphages was used as the model wastewater. A set of 12 experiments were conducted separately for both model organisms (to prevent the phages from feeding on *E.coli*) to investigate the effects of charge dosage and CDR on their removal. For simplicity, the experiments with demi water have been identified as phase 1 experiment. The various operational parameters maintained during the experiment are shown in Table 4

Table 4 Operational parameters for phase-1 experiments

Microbial indicator	Current (A)	Electrode area (cm <sup>2</sup> )	Volume (L)	Current density (mA/cm <sup>2</sup> )	Charge dosage (C/L)	Charge dosage rate (C/L/min)	EC time (min)	Fe <sub>theo</sub> generated (mg/L)
WR1 E.coli / $\phi$ X174 Somatic coliphage	0.06	32	0.5	2	50	7.2	6.94	14.5
	0.06	32	0.5	2	75	7.2	10.42	21.8
	0.06	32	0.5	2	150	7.2	20.83	43.5
	0.06	32	0.5	2	200	7.2	27.78	58.0
	0.3	32	0.5	10	50	36	1.39	14.5
	0.3	32	0.5	10	75	36	2.08	21.8
	0.3	32	0.5	10	150	36	4.17	43.5
	0.3	32	0.5	10	200	36	5.56	58.0
	0.6	32	0.5	20	50	72	0.69	14.5
	0.6	32	0.5	20	75	72	1.04	21.8
	0.6	32	0.5	20	150	72	2.08	43.5
	0.6	32	0.5	20	200	72	2.78	58.0

.For the next set of experiments in phase 2, synthetic wastewater effluent as explained in section 3.2 was prepared and spiked with the same model organisms. A total of 20 experiments were conducted in the same way as phase 1. Along with microbial attenuation, co-removal of phosphorus and nitrogen at different charge dosage and CDRs was investigated. The operational parameters were slightly extended with the addition of a lower CDR of 5 C/L/min and charge dosage of 10 C/L. The experimental conditions are summarized in Table 5.

Table 5 Operational parameters of phase-2 experiments

Microbial indicator	Current (A)	Electrode area (cm <sup>2</sup> )	Volume (L)	Current density (mA/cm <sup>2</sup> )	Charge dosage (C/L)	Charge dosage rate (C/L/min)	EC time (min)	Fe <sub>theo</sub> generated (mg/L)
WR1 E.coli / $\phi$ X174 Somatic coliphage	0.04	32	0.5	1	10	5	2.0	2.90
	0.04	32	0.5	1	50	5	10.0	14.51
	0.04	32	0.5	1	75	5	15.0	21.76
	0.04	32	0.5	1	150	5	30.0	43.88
	0.04	32	0.5	1	200	5	40.0	58.04
	0.06	32	0.5	2	10	7.2	1.4	2.90
	0.06	32	0.5	2	50	7.2	6.9	14.51
	0.06	32	0.5	2	75	7.2	10.4	21.76
	0.06	32	0.5	2	150	7.2	20.8	43.88
	0.06	32	0.5	2	200	7.2	27.8	58.04
	0.30	32	0.5	10	10	36	0.3	2.90
	0.30	32	0.5	10	50	36	1.4	14.51
	0.30	32	0.5	10	75	36	2.1	21.76
	0.30	32	0.5	10	150	36	4.2	43.88
	0.30	32	0.5	10	200	36	5.6	58.04
	0.60	32	0.5	20	10	72	0.1	2.90
	0.60	32	0.5	20	50	72	0.7	14.51
	0.60	32	0.5	20	75	72	1.0	21.76
	0.60	32	0.5	20	150	72	2.1	43.88
	0.60	32	0.5	20	200	72	2.8	58.04

In the final phase, real wastewater effluent from a Dutch activated sludge wastewater treatment plant without disinfection was subjected to different charge dosages and CDRs based on the results obtained in phase1 and 2. The investigation was carried out for the removal of pathogen indicators such as – *E.coli*, *ESBL E.coli*, Enterococci, VRE, Somatic coliphages and *Clostridium perfringens* spores, along with COD, TSS, TN, NO<sub>2</sub><sup>-</sup>, NO<sub>3</sub><sup>2-</sup>, NH<sub>4</sub><sup>+</sup> and PO<sub>4</sub><sup>3-</sup>, turbidity and color. The experimental conditions are summarized in Table 6.

Table 6 Operational parameters of phase-3 experiments

Pollutant type	Current (A)	Electrode area (cm <sup>2</sup> )	Volume (L)	Current density (mA/cm <sup>2</sup> )	Charge dosage (C/L)	Charge dosage rate (C/L/min)	EC time (min)	Fe <sub>theo</sub> generated (mg/L)
Physical, chemical and biological parameters	0.10	32	1	3.12	50	7.2	6.94	14.51
	0.10	32	1	3.12	100	7.2	13.80	29.02
	0.10	32	1	3.12	200	7.2	27.78	58.04
	0.10	32	1	3.12	400	7.2	55.50	116.08
	0.60	40	1	15	50	36	1.39	14.51
	0.60	40	1	15	100	36	2.78	29.02
	0.60	40	1	15	200	36	5.56	58.04
	0.60	40	1	15	400	36	11.11	116.08

### 3.7 Treatment cost

The operating cost of EC process is encompassed of electrodes and electrical energy costs along with labour, maintenance, sludge dewatering and disposal. In this study, energy and electrode material usage are considered for major expenses in calculating the operating cost (€/m<sup>3</sup>). The operating cost is calculated as shown in Equation 6 (Khaled et al., 2015).

$$\text{Operating cost} = a C_{\text{energy}} + b C_{\text{electrode}} \quad \text{- Equation 6}$$

where,  $a$  is the energy cost = 0.1707 €/kWh (Eurostat, 2019),  $b$  is steel S235 cost = 0.21 €/kg (MEPS International Ltd, 2019),  $C_{\text{energy}}$  (kWh/m<sup>3</sup>) and  $C_{\text{electrode}}$  (kg/m<sup>3</sup>) are the consumption quantities at different charge dosages and CDRs.

Electrical energy consumption is calculated as shown in Equation 7.

$$C_{\text{energy}}(\text{kWh}/\text{m}^3) = \frac{U \times I \times t}{V} \quad \text{- Equation 7}$$

where  $U$  is the voltage cell (V),  $I$  is the current (A),  $t$  is the treatment time (h) and  $V$  is the volume of wastewater treated (m<sup>3</sup>).

Electrode material consumption (kg/m<sup>3</sup>) is calculated according to Faraday's Law as shown in Equation 8.

$$C_{electrodes}(kg/m^3) = \frac{I \times t \times M}{n \times F \times V}$$

- Equation 8

where I is the current (A), t is treatment time (s), M is the molecular mass of iron (55.84 g/mol), z is the number of electrons transferred (z = 2), F is the Faraday's constant (96487 C/mol) and V is volume (m<sup>3</sup>).

## Chapter-4

## Results

The results of various experiments conducted along the course of the investigation are presented in this chapter and are grouped according to the type of water matrix used, namely: demineralized water, synthetic wastewater effluent and real wastewater effluent.

### 4.1 Evolution of pH

During the course of the experiment, pH increased due to the dissolution of hydroxyl ions from the cathode. On switching off the current i.e., when the hydroxyl ions were no longer released, pH dropped close to the initial value. Considering the initial pH range of 7-7.5, the final pH in demi water and synthetic wastewater effluent increased up to 8.5 at high charge dosage of 400 C/L. Whereas in real wastewater effluent, the highest pH observed was 7.8 at 400 C/L. These results indicated that the final pH depended on the type of water matrix used.

Figures 11, 12 and 13 show the initial and final pH in the influent and bulk sample as a function of charge dosage in demi water, synthetic wastewater effluent and real wastewater effluent respectively. The initial and final pH measured at the beginning and end of the experiment is indicated at 0 C/L and at corresponding charge dosages respectively.

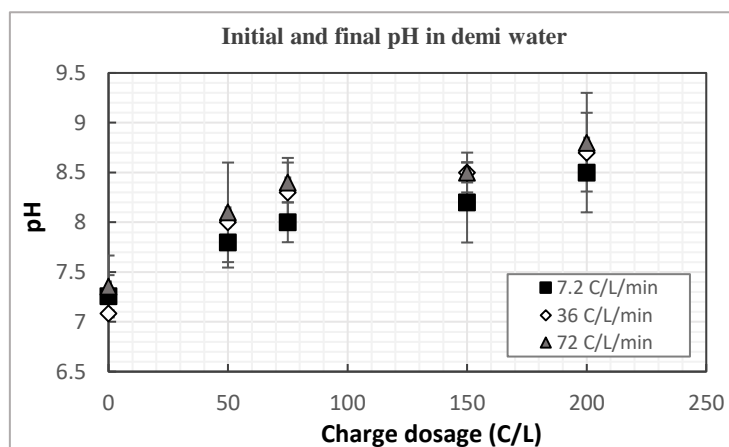


Figure 11 Initial and final pH in demi water as a function of charge dosage

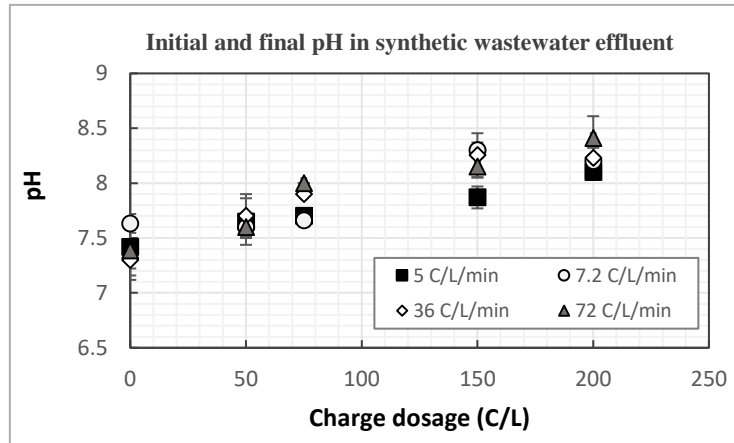


Figure 12 Initial and final pH in synthetic wastewater effluent as a function of charge dosage

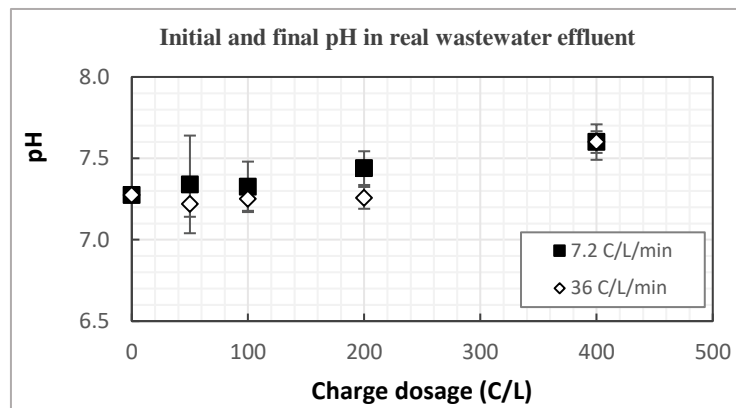


Figure 13 Initial and final pH in real wastewater effluent as a function of charge dosage

## 4.2 Iron dissolution

Iron dissolution during EC was analyzed in both bulk and supernatant samples of real wastewater effluent. The theoretical ( $Fe_{theo}$ ) and experimental ( $Fe_{exp}$ ) iron concentration as a function of charge dosage are shown in Table 7. Fe dissolution increased with increasing charge dosage irrespective of the variation in CDRs.  $Fe_{exp}$  was slightly higher than  $Fe_{theo}$  predicted using Faraday's law may be due to anomalous pitting corrosion behaviour of iron and the rapid oxidation of oxide film formed on the electrode surface. As a result of these electrochemical reactions, the amount of Fe species and iron hydroxides can be produced greater than expected (predicted by Faraday's law) resulting in an average FE of 114.8%.

Table 7 Theoretical and experimental iron (mg/L) in real wastewater effluent

Charge dosage (C/L)	Fe <sub>theo</sub> (mg/L)	Fe <sub>exp</sub> (mg/L)
50	14.51	16.58
100	29.02	32.28
200	58.04	65.38
400	116.08	140.99

After the flocculation phase, iron concentration in supernatant reduced with increasing charge dosage as shown in Figure 14. The supernatant contained 13.5 mg/L of iron at charge dosage of 50 C/L and 4.8 mg/L at high charge dosage of 400 C/L. The generated coagulants before and after flocculation phase are shown in Figure 15.

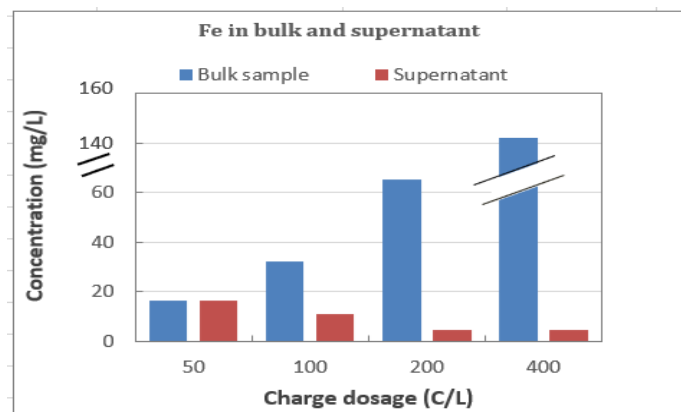


Figure 14 Iron concentration in bulk and supernatant of real wastewater effluent

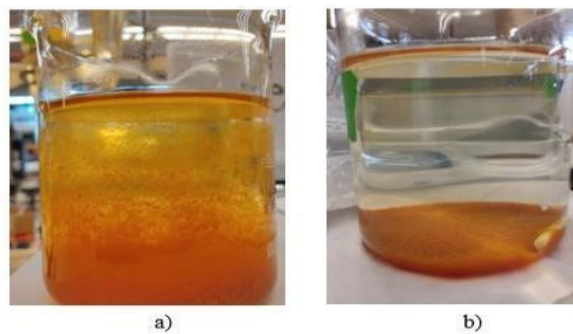


Figure 15 Iron precipitates, a) before flocculation b) after flocculation in real wastewater effluent

### 4.3 Effect of current density

The amount of iron produced in the wastewater during EC depended on the duration of the current passed which was determined by the current density. A high current density allowed a shorter treatment time compared to a low current density i.e., passing the same amount of charge in a shorter duration. WR1 *E.coli* removal increased with increasing iron dosage, but the removal rate was altered by the applied current density.

The significant impact of current densities of 1, 2, 10 and 20 mA/cm<sup>2</sup> on WR1 *E.coli* attenuation in synthetic wastewater effluent is shown in Figure 16. The six data points corresponding to each current density signifies the increase in iron production (at charge dosages of 10, 20, 50, 75, 150 and 200 C/L) with increasing treatment time. The highest removal observed was 4.3, 4.1, 3.9 and 4.2 log units at treatment durations of 40, 27, 5.3 and 2.7 min for current densities of 1, 2, 10 and 20 mA/cm<sup>2</sup> respectively. These results obtained after overnight settling show that the removal is not influenced by the current density (i.e., treatment time) but by the charge dosage (i.e., iron production).

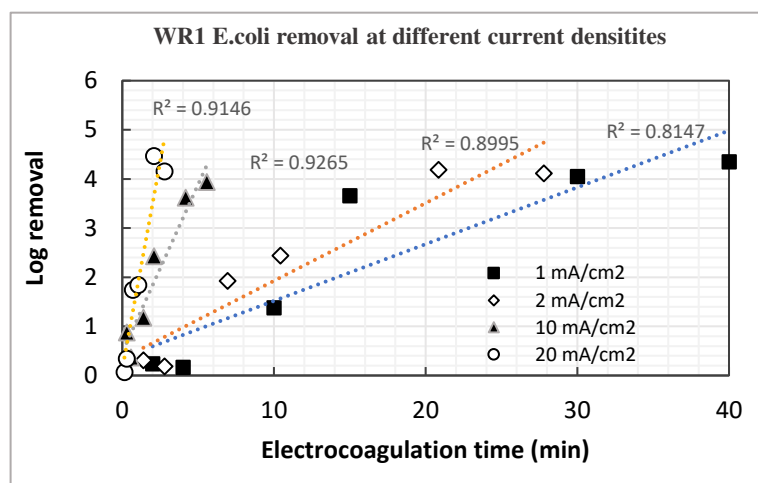


Figure 16 Effect of current density on WR1 *E.coli* removal in synthetic wastewater effluent

### 4.4 Effect of charge dosage and charge dosage rate (CDR) on microbial attenuation

#### 4.4.1 Demineralized water

The removal of WR1 *E.coli* increased with increasing charge dosage as discussed in Section 4.3 and was the highest at the lowest CDR. The highest removal of 6.8 log units was observed for WR1 *E. coli* at 200 C/L and 7.2 C/L/min. A poor removal of  $\phi$ X174 Somatic coliphages was observed with 0.7 log at 200 C/L and 7.2 C/L/min. These results confirmed the effectiveness of Fe-EC on microbial attenuation (specifically bacteria) in demi water.

Figure 17 a) and b) shows the removal of *WR1 E. coli* and  $\phi$ X174 Somatic coliphages respectively in demi-water as a function of charge dosage at CDRs of 7.2, 36 and 72 C/L/min.

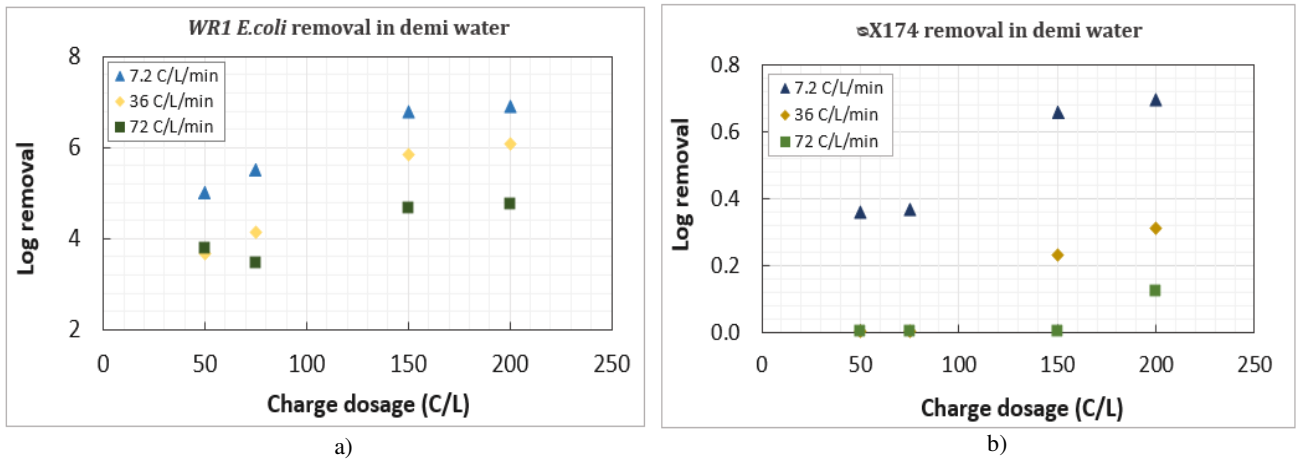


Figure 17 Removal of a) *WR1 E. coli* removal and b)  $\phi$ X174 Somatic coliphages in demi water

#### 4.4.2 Synthetic wastewater effluent

The removal of *WR1 E. coli* and  $\phi$ X174 Somatic coliphages followed different trends in synthetic wastewater effluent compared to demi water. In the presence of synthetic wastewater constituents, the removal of *WR1 E. coli* reduced slightly, while  $\phi$ X174 Somatic coliphages removal improved drastically. The investigation for *WR1 E. coli* in experiment 1 showed the highest removal values of 4.5, 4.4, 3.7 and 3.2 log units at CDRs of 5, 7.2, 36 and 72 C/L/min and charge dosage of 200 C/L. In experiment 2, the highest removal values observed were 5.4, 4.7, 5.1 and 4.9 log units at 5, 7.2, 36 and 72 C/L/min and 200 C/L.

Figures 18 a) and b) show the removal of *WR1 E. coli* in experiment 1 and 2 respectively. The removal was higher in experiment 2 due to change in concentration of N and P. However, the highest removal in both the experiments was prominent at 5 C/L/min for most of the charge dosages.

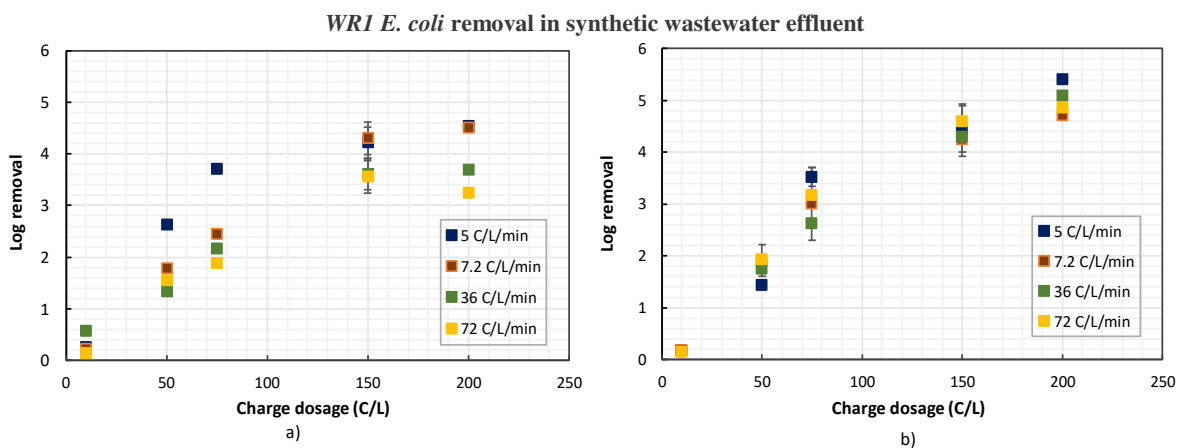


Figure 18 *WR1 E. coli* removal in synthetic wastewater effluent in (a) Experiment-1 and (b) Experiment-2

$\phi$ X174 Somatic coliphages removal increased in both experiment 1 and 2. Unlike the trend of *WRI E. coli*, the removal was higher in experiment 1 than in experiment 2. The highest removal values observed in experiment 1 were 4.6 log units at 5 and 7.2 C/L/min and 3.7 log units at 36 and 72 C/L/min and at charge dosage 200 C/L. In experiment 2, removal of 3.9, 3.5, 3.4 and 3.3 log units was observed at 5, 7.2, 36 and 72 C/L/min and at 200 C/L.

Figure 19 a) and b) shows the removal of  $\phi$ X174 Somatic coliphages in experiment 1 and 2 respectively. The removal at 150 and 200 C/L was the highest at low CDR of 5 and 7.2 C/L/min.

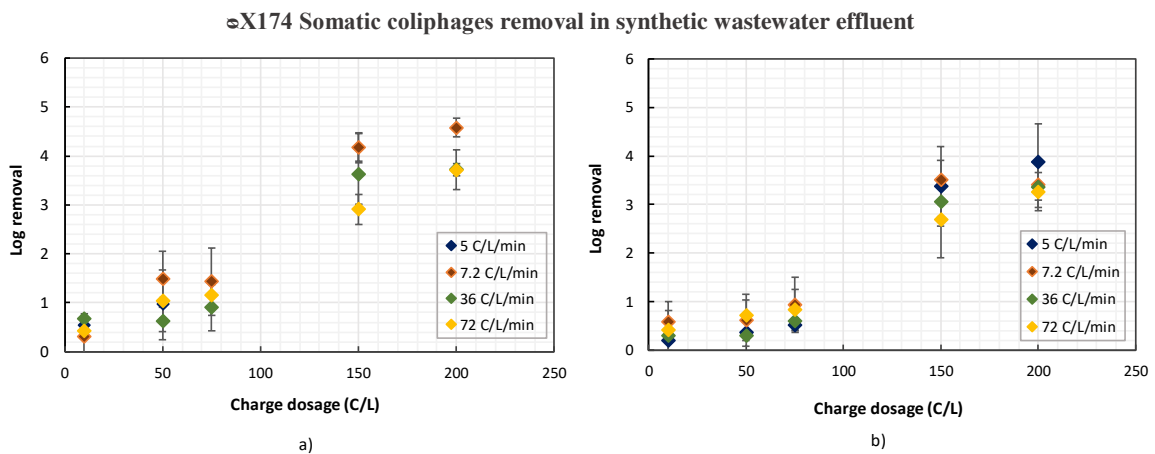


Figure 19  $\phi$  X174 removal in synthetic wastewater effluent in (a) Experiment-1 and (b) Experiment-2

#### 4.4.3 Municipal wastewater effluent

##### 4.4.3.1 Attenuation of *E. coli*, *ESBL E. coli*, Enterococci and VRE

The attenuation of *E. coli*, *ESBL E. coli*, Enterococci and VRE was investigated in real wastewater effluent. The removal increased with increasing charge dosage and slow charge dosage rate as observed in demi water and synthetic wastewater effluent.

At 7.2 C/L/min, the highest removal values for *E. coli*, Enterococci, *ESBL E. coli* and VRE were 3.7, 3.6,  $\geq 2.6$  and  $\geq 2.5$  log units respectively at 400 C/L. The values for *ESBL E. coli* and VRE at 200 C/L and 400 C/L are reported as 2.6 and 2.5 log units respectively as their concentration in the supernatant was below the detection limit. Unfortunately, a larger sample volume was not available to perform the analysis due to insufficient assay volume. Figure 20 shows the removal of *E. coli*, *ESBL E. coli*, Enterococci and VRE in real wastewater effluent at CDR of 7.2 C/L/min.

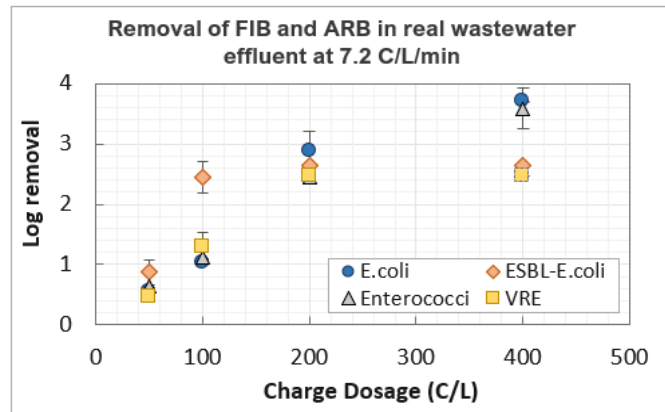


Figure 20 *E.coli*, *Enterococci*, *ESBL E.coli* and *VRE* removal in real wastewater effluent at 7.2 C/L/min

At 36 C/L/min, the highest removal values were 2.5, 2.6,  $\geq 2$  and  $\geq 2.1$  log units for *E.coli*, *Enterococci*, *ESBL E. coli* and *VRE* respectively. The removal values of *ESBL E. coli* and *VRE* at 200 C/L and 400 C/L are reported as 2 and 2.1 log units as their concentration in the supernatant were below the detection limit as observed for 7.2 C/L/min. Figure 21 shows the removal of *E. coli*, *ESBL E. coli*, *Enterococci* and *VRE* in real wastewater effluent at CDR of 36 C/L/min.

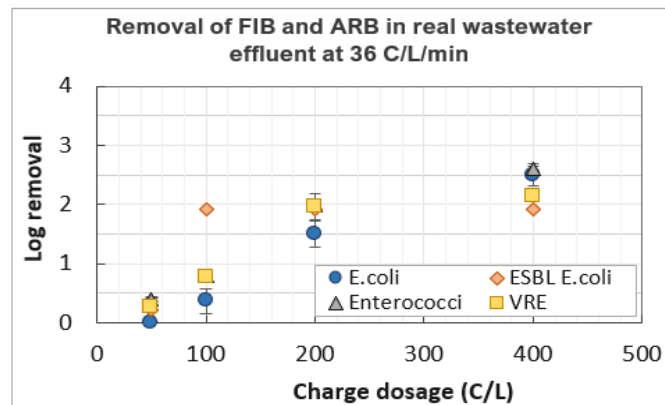


Figure 21 *E.coli*, *Enterococci*, *ESBL E.coli* and *VRE* removal in real wastewater effluent at 36 C/L/min

#### 4.4.3.2 Attenuation of Somatic coliphages

Removal of Somatic coliphages increased with increment in iron concentration and was similar at both CDRs of 7.2 and 36 C/L/min. The removal at 400 C/L and 7.2 C/L/min was reported as 2.3 log units as their concentration in the supernatant was below the detection limit. The highest removal values observed at 400 C/L were  $\geq 2.3$  and 2 log units at 7.2 and 36 C/L/min respectively. Figure 22 shows the removal of Somatic coliphages in real wastewater effluent at 7.2 and 36 C/L/min.

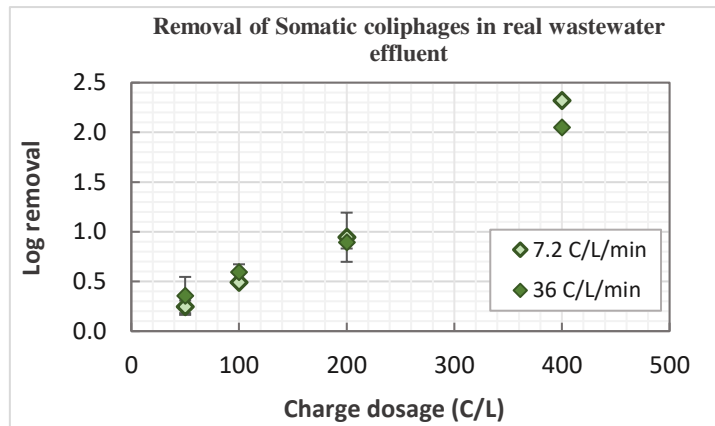


Figure 22 Somatic coliphages removal in real wastewater effluent

#### 4.4.3.3 Attenuation of *Clostridium perfringens* spores

*C. perfringens* spores removal increased with increasing charge dosage until 200 C/L after which the graph depicted a tailing phenomenon. Low CDR of 7.2 C/L/min showed a higher removal until 100 C/L beyond which the removal was higher at 36 C/L/min. The highest removal was observed to be 2.1 and 2.7 log units at 400 C/L and 7.2 C/L/min and 36 C/L/min respectively. Figure 23 shows the removal of *C. perfringens* spores in real wastewater effluent at 7.2 and 36 C/L/min.

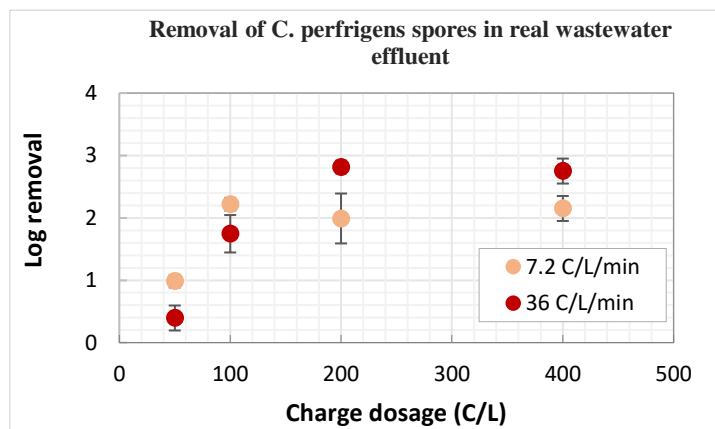


Figure 23 *C. perfringens* spores removal in real wastewater effluent

## 4.5 Removal of wastewater quality parameters

This section shows the observations for the reduction of wastewater quality parameters in synthetic wastewater effluent and real wastewater effluent.

### 4.5.1 Synthetic municipal wastewater effluent

#### 4.5.1.1 Phosphorous

Phosphorous significantly reduced with increasing charge dosage. The removal was similar in both the experiments indicating the efficiency to be independent of the initial concentration. The highest removal values were 98.5% and 99% in experiment 1 and 2 respectively at 200 C/L and at all CDRs of 5, 7.2, 36 and 72 C/L/min. However, in experiment 2 the effect of CDR was prominent until 75 C/L beyond which it was similar at all CDRs.

Figures 24 and 25 show phosphorous removal percentage as a function of charge dosage in synthetic wastewater effluent in experiments 1 and 2 respectively.

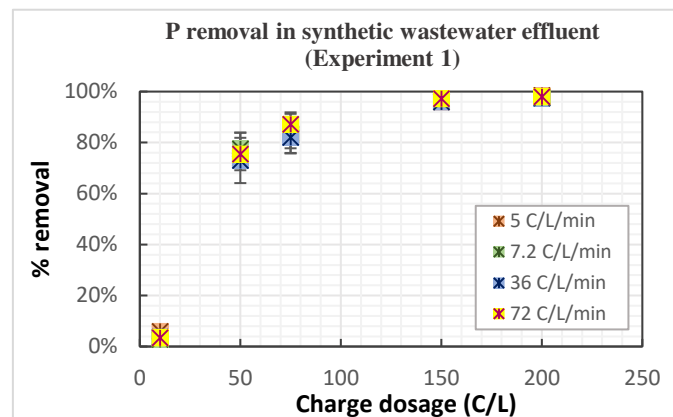


Figure 24 Phosphorous removal in experiment 1 with synthetic wastewater effluent

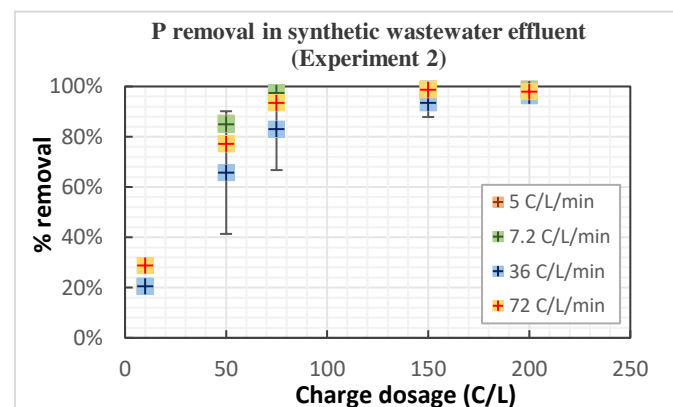


Figure 25 Phosphorous removal in experiment 2 with synthetic wastewater effluent

#### 4.5.1.2 Total nitrogen

Unlike phosphorus removal, TN removal decreased with increasing iron dosage. The highest removal occurred at the lowest charge dosage of 10 C/L and gradually reduced with increasing dosage. In experiment 1, the highest removals were 88%, 94%, 90% and 94% at 10 C/L and CDRs of 5, 7.2, 36 and 72 C/L/min respectively. In experiment 2, the same trend was observed with the removal of 87%, 89%, 83% and 85% at 10 C/L at CDRs of 5, 7.2, 36 and 72 C/L/min respectively.

Figure 26 and 27 shows the decrease in TN removal efficiency with increasing charge dosage in synthetic wastewater effluent in experiment 1 and 2 respectively.

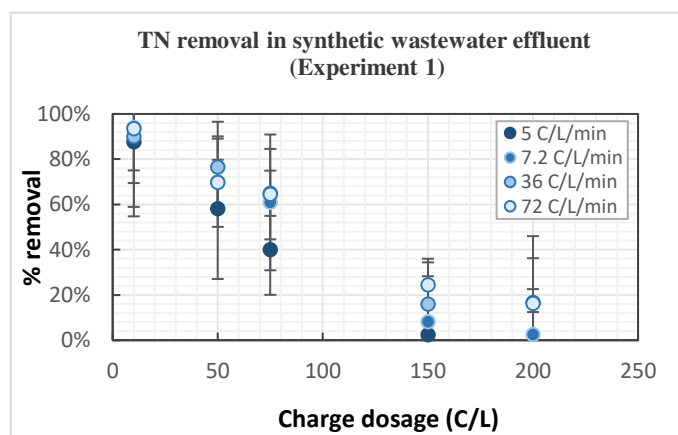


Figure 26 Total nitrogen removal in experiment 1 with synthetic wastewater effluent

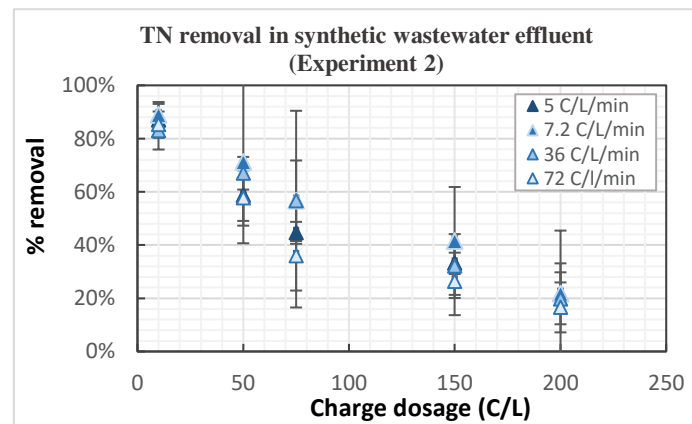


Figure 27 Total nitrogen removal in experiment 2 with synthetic wastewater effluent

## 4.5.2 Municipal wastewater effluent

### 4.5.2.1 Phosphorous

Phosphorous removal followed the same trend as observed in synthetic wastewater effluent. The removal was effective with increasing iron dosage. The highest removal observed was 99% at 400 C/L and CDRs of 7.2 and 36 C/L/min as shown in Figure 28.

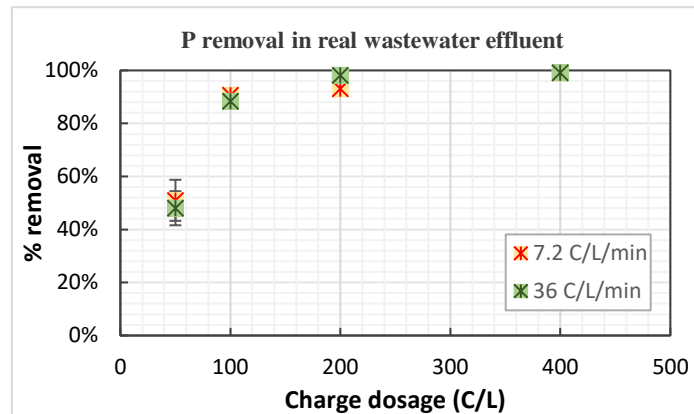


Figure 28 Phosphorous removal in real wastewater effluent

### 4.5.2.2 Total nitrogen

The trend for TN removal in real wastewater effluent differed from that of synthetic wastewater effluent. This can be due to the use of urea in the synthetic composition which contributed to organic N source. In real effluent, the presence of organic and inorganic N shows a different behavior during treatment. Inorganic N species:  $\text{NO}_3^-$ ,  $\text{NO}_2^-$  and  $\text{NH}_4^+$  were measured to see changes in their concentration. The major reduction in TN was observed to be by organic N on comparing their removals with inorganic N. Figure 29 shows the removal of TN with increasing charge dosage. The removal was very low with 13% and 8% at 400 C/L and 36 and 7.2 C/L/min respectively.

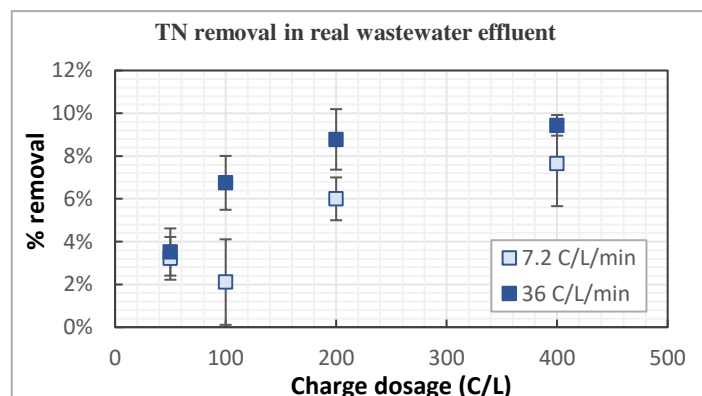


Figure 29 Total nitrogen removal in real wastewater effluent

The analysis post-treatment showed a reduction in  $\text{NO}_3^-$  concentration with increasing treatment time resulting in a minute increase in  $\text{NO}_2^-$  and  $\text{NH}_4^+$  at 7.2 and 26 C/L/min as shown in Figure 30 a) and b) respectively. At 7.2 C/L/min,  $\text{NO}_3^-$  reduced by 5% with an increase in  $\text{NH}_4^+$  and  $\text{NO}_2^-$  by 11% and 6% respectively at 400 C/L. Whereas at 36 C/L/min,  $\text{NO}_3^-$  and  $\text{NO}_2^-$  were reduced by 14% and 3% respectively and  $\text{NH}_4^+$  increased by 4% at 400 C/L. The observation here is that the decrease in  $\text{NO}_3^-$  was higher at 36 C/L/min than 7.2 C/L/min.

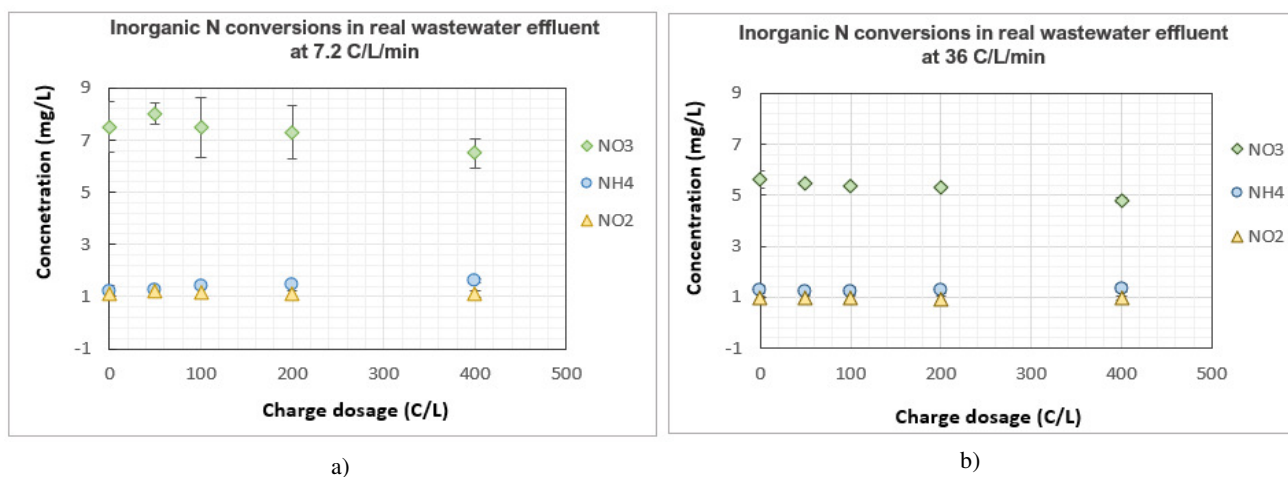


Figure 30  $\text{NO}_3^-$ ,  $\text{NO}_2^-$  and  $\text{NH}_4^+$  conversions in real wastewater effluent at a) 7.2 C/L/min and b) 36 C/L/min

Comparison of organic and inorganic N reduction showed the major removal by organic N. The effect of CDR was evident at charge dosage of 200 and 400 C/L, resulting in a higher removal at 36 C/L/min than 7.2 C/L/min as shown in Figure 31.

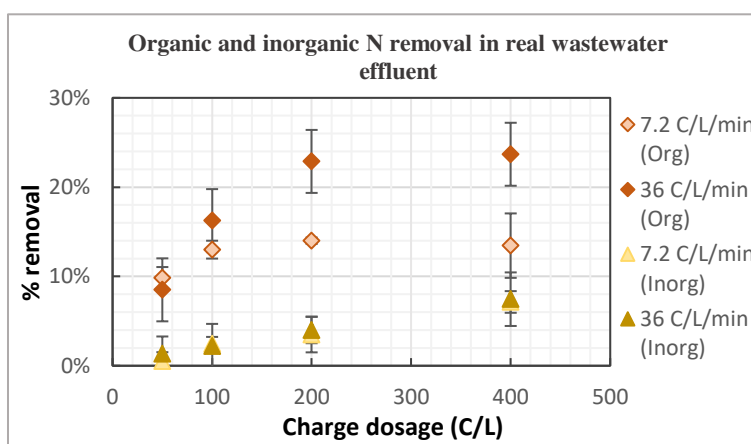


Figure 31 Organic and inorganic nitrogen removal percentage in real wastewater effluent

### 4.5.2.3 Chemical Oxygen demand

COD concentration reduced with increasing charge dosage over time. The reduction was higher at CDR of 36 C/L/min than 7.2 C/L/min. The concentration graph in Figure 32a) shows the lowest concentration that can be reached to be around 30 mg /L irrespective of their different initial concentration.

The highest removal percentages were 47% and 34% at 400 C/L and 36 and 7.2 C/L/min as shown in Figure 32 b). This difference in percentage is due to the initial COD concentration, however, the final COD value shows the removal to be similar at both CDRs.

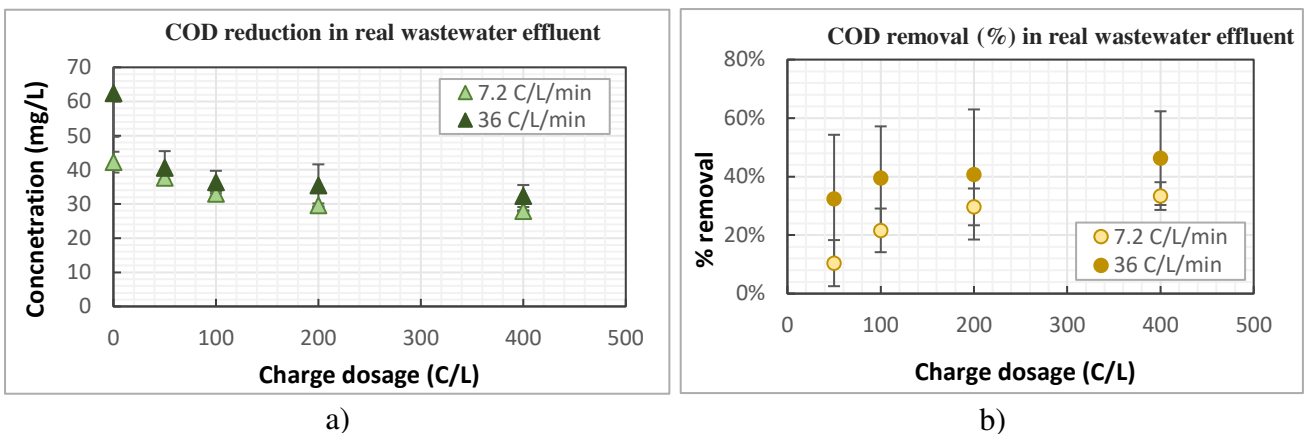


Figure 32 Reduction in COD concentration (a) and removal percentage (b) in real wastewater effluent

### 4.5.2.4 Total suspended solids

TSS concentration in the real wastewater effluent was between 2-4 mg/L and increased upon dosing iron. At 7.2 C/L/min the concentration increased to 28 mg/L at 50 C/L and gradually decreased to 7 mg/L at 400 C/L. While at 36 C/L/min the concentration increased to 16 mg/L at 50 C/L and decreased to 8 mg/L at 400 C/L. The final concentration was close to the initial at both CDRs as shown in Figure 33.

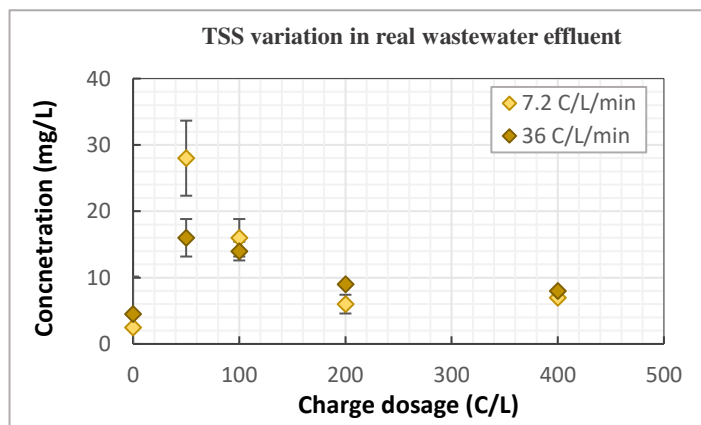


Figure 33 Variation in TSS concentration in real wastewater effluent

#### 4.5.2.5 Turbidity

Turbidity observed an increase similar to that of TSS. The initial concentration was 1.1-1.7 NTU which was very low. With an increase in iron dosage, turbidity increased to 7.2 NTU at 50 C/L and dropped to 6.6 NTU at 400 C/L at 7.2 C/L/min. While at 36 C/L, the decrease was from 12 NTU at 50 C/L to 4 NTU at 400 C/L. Figure 34 shows the variation in turbidity in real wastewater effluent and the reduction in final concentration despite the variable increase at 50 C/L at both CDRs.

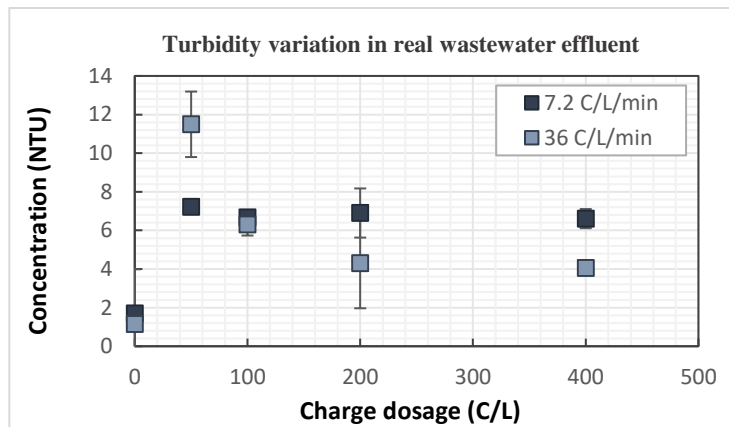


Figure 34 Variation in turbidity in real wastewater effluent

#### 4.5.2.6 Color

The release of hydroxides upon electrodes dissolution contributed to turbidity which portrayed a false reading of color. For this reason, the supernatant was filtered using a 0.45 $\mu$ m filter to assess true color. This resulted overall in the highest removal efficiency of 76% and 33% at 400 C/L and 36 and 7.2 C/L/min respectively as shown in Figure 35.

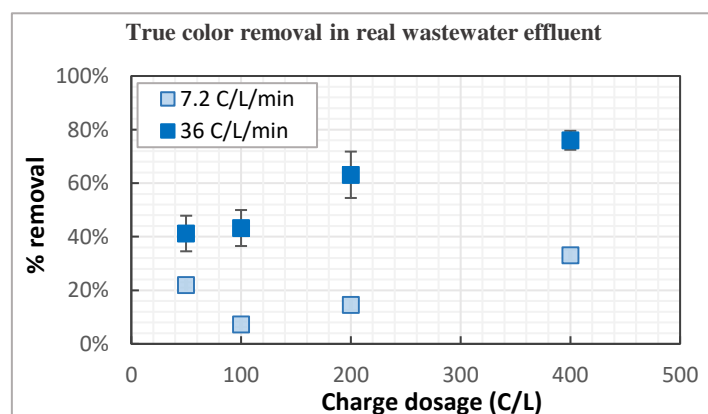


Figure 35 True color reduction in real wastewater effluent

#### 4.5.2.7 Chloride

Chloride concentration was measured before and after EC in real wastewater effluent to observe the occurrence of chloride ions oxidation during EC. The influent concentration was 110-117 mg/L and post-treatment a slight variation (within the error range) of 0.4-1.3% was observed at all charge dosages and CDRs indicating no major variation in concentration.

#### 4.6 Sludge characterization

The sludge produced during EC with real and synthetic wastewater effluent was characterized to know its composition due to a wide range of CDRs used. The rate at which the coagulants were dosed determined the flocs separation mechanisms, in terms of sedimentation and floatation.

At low CDR of 7.2 C/L/min sedimentation of flocs over time was observed as shown in Figure 36 a). At intermediate and high CDR of 36 and 72 C/L/min, excess hydrogen gas released at the cathode resulted in separation by floatation as seen in Figure 36 b). These floating flocs were made to settle by slowly mixing with a sterile stirrer or the hydrogen bubbles were destroyed when the treated water was transferred to an Imhoff cone allowing the flocs to settle at the bottom. Figure 36 c) shows the hydrogen bubbles formed at 36 and 72 C/L/min due to rapid electrode dissolution.

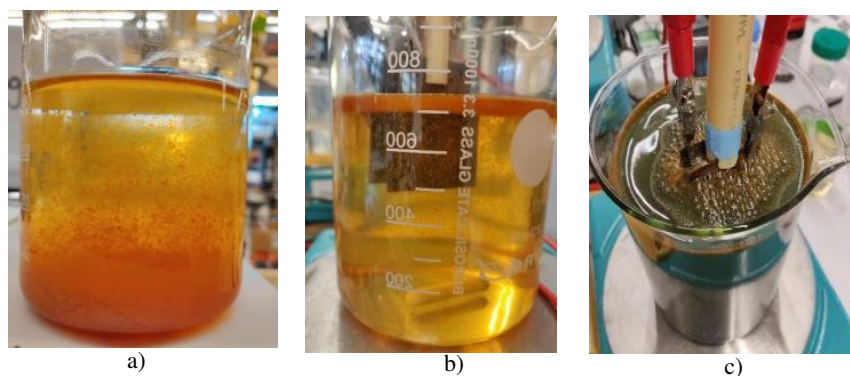


Figure 36 (a) Floc sedimentation (b) floatation and (c) bubbles due to the release of hydrogen gas in synthetic wastewater effluent

The flocs formed at high and low CDRs differed in terms of their physical structure. At slow iron dosing the flocs were voluminous, irregular shaped, porous and prone to restructuring and compaction. At rapid dosage flocs were dense, compact structures less prone to shear stress over longer flocculation times like those generated in chemical coagulation, suitable for processes incorporating higher shear environments. The difference in floc structures at 7.2 and 36 C/L/min is shown in Figure 37 a) and b) respectively.

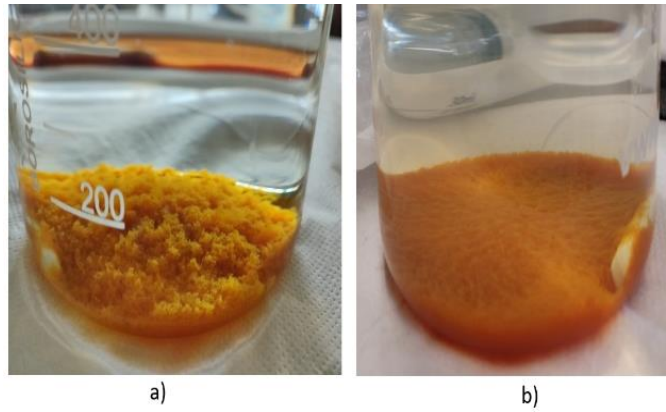


Figure 37 Floc structures formed at CDRs of 7.2 C/L/min (a) and 36 C/L/min (b) in real wastewater effluent

Characterization of sludge (in real wastewater effluent) using XRD confirmed the formation of Calcite ( $\text{CaCO}_3$ ) at 50, 100 and 200 C/L at both CDRs of 7.2 and 36 C/L/min. Along with calcite, iron hydroxides were formed, but could not be detected by XRD as they lacked a crystalline structure. At 400 C/L, Goethite ( $\alpha\text{Fe}^{3+}\text{O}(\text{OH})$ ) was formed by the transformation of poorly crystalline Fe minerals at 7.2 C/L/min, whereas both calcite and goethite were formed at 36 C/L/min.

Figure 38 shows the formation of iron hydroxide (a) and goethite (b) at low and high charge dosage of 100 and 400 C/L respectively. The dark brown colored sludge containing goethite was observed to be attracted by a magnet.

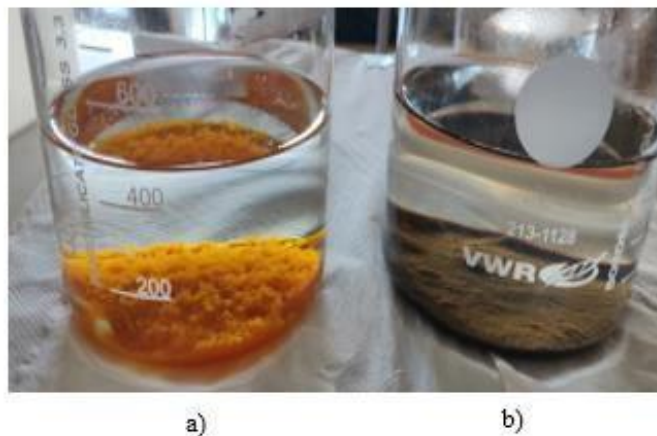


Figure 38 Characterization of EC sludge: (a) Iron hydroxide at 100 C/L and (b) Goethite at 400 C/L in real wastewater effluent.

#### 4.7 Removal kinetics

The removal of pathogen indicators *E.coli*, Enterococci, *Clostridium perfringens* spores and Somatic coliphages was studied at different charge dosages and CDRs as discussed in section 4.4.3. The results showed a log-linear relation between the removal of micro-organisms and increasing charge dosage. Hence the kinetic parameters for microbial removal against charge dosage of 50, 100, 200 and 400 C/L is obtained with a log-linear model at CDRs of 7.2 and 36 C/L/min as shown in Equation 9.

$$\log \frac{C_0}{C_t} = k \times CD \quad \text{- Equation 9}$$

where,  $C_0$  is the initial microbial concentration before treatment (cfu/ml) and  $C_t$  is the final microbial concentration after treatment at a particular charge dosage (cfu/ml),  $k$  is the rate constant and  $CD$  is the charge dosage in C/L.

Since the removal of *E.coli* and Enterococci was similar, *E.coli* data is used to represent the removal of fecal indicator bacteria. The rate constants obtained for *E.coli* are  $0.0095 \text{ (C/L)}^{-1}$  and  $0.0054 \text{ (C/L)}^{-1}$  at CDRs of 7.2 and 36 C/L/min respectively. The removal rate is slightly higher at 7.2 C/L/min indicating a higher removal during slow dosing of iron. Figure 39 a) and b) shows the linear relation between the removal of *E.coli* and charge dosage at 7.2 and 36 C/L/min respectively.

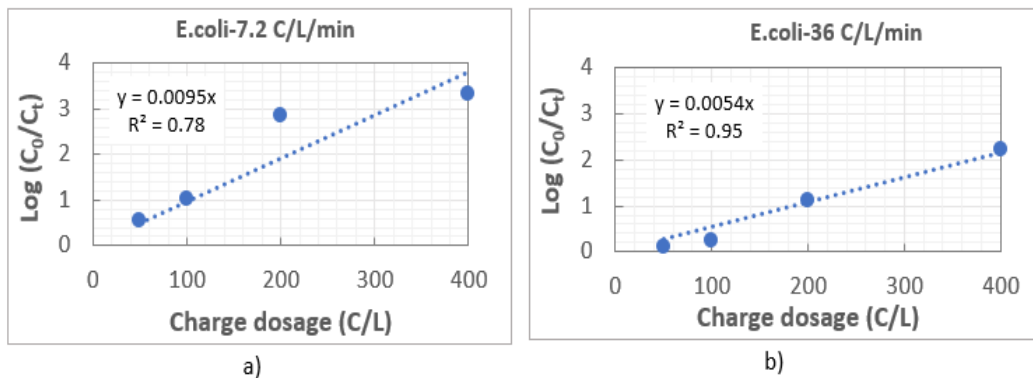


Figure 39 Log-linear relation between removal of *E.coli* and charge dosage at a) 7.2 C/L/min and b) 36 C/L/min

The removal of *C. perfringens* spores increased linearly with charge dosage until 100 C/L and 200 C/L at 7.2 and 36 C/L/min respectively after which a tailing was observed. Hence, the removal of linear and tailing trend has been modelled separately. At 7.2 C/L/min, the rate constant is  $0.0217 \text{ (C/L)}^{-1}$  for the linear trend until 100 C/L and  $-8\text{E-}05 \text{ (C/L)}^{-1}$  for the tailing trend from 100 to 400 C/L. The very low rate constant for the tail indicates a poor removal rate compared to the linear trend. While at 36 C/L/min, the rate constant is  $0.013 \text{ (C/L)}^{-1}$  until 200 C/L beyond which the rate reduces to  $-3\text{E-}04 \text{ (C/L)}^{-1}$  indicating a very low removal rate.

Figure 40 a) and b) shows the log-linear relationship between the removal of *C. perfringens* spores and charge dosage at 7.2 and 36 C/L/min respectively.

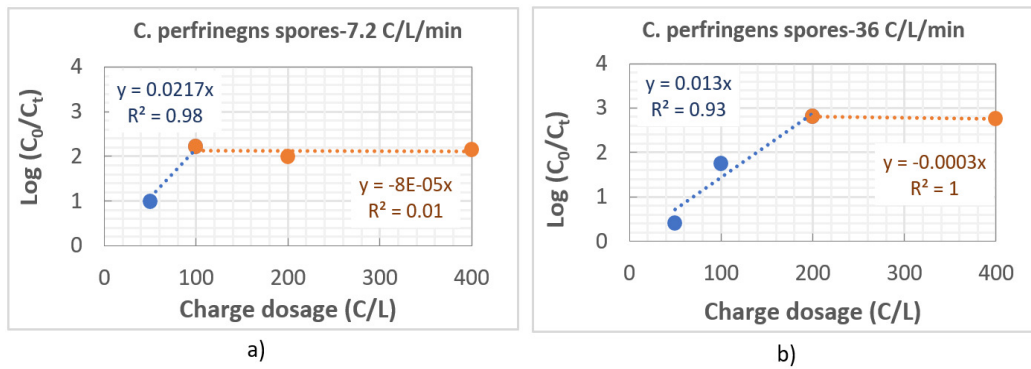


Figure 40 Log-linear relation between removal of *C. perfringens* spores and charge dosage at a) 7.2 C/L/min and b) 36 C/L/min

Somatic coliphages removal showed a strong linear relation with increasing charge dosage. The rate constants were similar with  $0.0056 \text{ (C/L)}^{-1}$  at 7.2 C/L/min and  $0.0050 \text{ (C/L)}^{-1}$  at 36 C/L/min. Figure 41 a) and b) shows the relation between somatic coliphages and charge dosage at 7.2 and 36 C/L/min respectively.

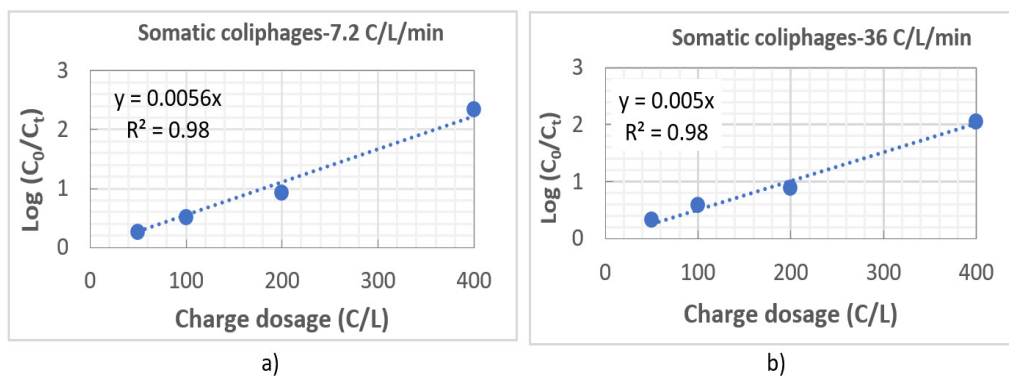


Figure 41 Log-linear relation between removal of Somatic coliphages and charge dosage at a) 7.2 C/L/min and b) 36 C/L/min

The parameters of the log-linear model for pathogen indicators *E.coli*, *C. perfringens* spores and Somatic coliphages at 7.2 and 36 C/L/min respectively are shown in Table 8.

Table 8 Parameters of log-linear model for removal of pathogen indicators as a function of charge dosage at different CDRs.

Indicator	$k \text{ (C/L)}^{-1}$		$R^2$	
	7.2	36	7.2	36
<i>E.coli</i>	0.0095	0.0054	0.78	0.95
<i>C. perfringens</i>	0.0217	0.0130	0.98	0.93
spores	-8.E-05	-3.E-04	0.01	1
Somatic Coliphages	0.0056	0.0050	0.98	0.98

## 4.8 Operating cost analysis

The major operating costs (€/m<sup>3</sup>) in terms of electrical energy cost (€/m<sup>3</sup>) and electrodes material cost (€/m<sup>3</sup>) at charge dosages of 50, 100, 200 and 400 C/L and CDRs of 7.2 and 36 C/L/min are shown in Table 9. The major contributor to the operating cost was the energy cost, which increased with the duration of the treatment and current intensity. The cost of electrode material depended exclusively on the charge dosage as it determined the iron released during the process. Also, the energy cost can vary tremendously from country to country depending on the cost of electricity. For example, the electricity cost can vary from 0.17 €/kWh in the Netherlands to 0.071€/kWh in India.

At CDR of 7.2 C/L/min, the current and the voltage used was 0.12 A and 7.5-7.7 volts respectively. This resulted in an operating cost of 0.02 €/m<sup>3</sup> at 50 C/L and 0.17 €/m<sup>3</sup> at 400 C/L. Whereas at 36 C/L/min, the current and the voltage was higher, 0.6 A and 26-28 volts respectively. This increased the operating cost to 0.07 €/m<sup>3</sup> at 50 C/L and 0.55 €/m<sup>3</sup> at 400 C/L.

The operating costs of EC obtained at the optimum charge dosage of 400 C/L and 7.2 C/L/min (0.17 €/m<sup>3</sup>) when compared with alternative tertiary treatment technologies such as Ozone (0.23 €/m<sup>3</sup>), UV (0.30 €/m<sup>3</sup>), Activated carbon (0.48 €/m<sup>3</sup>) and Reverse osmosis (0.65 €/m<sup>3</sup>) shows the ability of a cost-effective treatment (Bui et al., 2016).

Table 9 Cost of energy consumption, electrode material and operating at different charge dosages and CDRs in real wastewater effluent

Charge dosage (C/L)	Charge Dosage Rate (C/L/min)	Voltage(V)	Current (A)	Time (min)	Volume (m <sup>3</sup> )	C <sub>energy</sub> (€/m <sup>3</sup> )	C <sub>electrodes</sub> (€/m <sup>3</sup> )	Operating cost (€/m <sup>3</sup> )
50	7.2	7.5	0.12	6.94	0.001	0.02	0.003	0.02
100	7.2	7.5	0.12	13.89	0.001	0.04	0.006	0.04
200	7.2	7.6	0.12	27.78	0.001	0.07	0.012	0.08
400	7.2	7.7	0.12	55.56	0.001	0.15	0.024	0.17

Charge dosage (C/L)	Charge Dosage Rate (C/L/min)	Voltage(V)	Current (A)	Time (min)	Volume (m <sup>3</sup> )	C <sub>energy</sub> (€/m <sup>3</sup> )	C <sub>electrodes</sub> (€/m <sup>3</sup> )	Operating cost (€/m <sup>3</sup> )
50	36	26.5	0.6	1.39	0.001	0.06	0.003	0.07
100	36	27	0.6	2.78	0.001	0.13	0.006	0.13
200	36	27	0.6	5.56	0.001	0.26	0.012	0.27
400	36	28	0.6	11.11	0.001	0.53	0.024	0.55

#### **4.9 Comparison of treated water quality with reclaimed water guidelines**

The need to minimize health and environmental risks of water reuse has led to the development of regulations and guidelines for the safe use of treated wastewater in many countries. Some national and international organizations have developed reference standards for water reuse applications, because a reliable approach to the management of health and environmental risk from water reuse requires advanced guidance based on a majority consensus. Such guidance is provided in the form of risk management framework for the beneficial and sustainable management of water reuse systems. International organizations such as World Health organization (WHO), and national organization of federal governments such as US Environmental Protection Agency (US EPA) have provided guidelines which can be used by states that have limited , or no regulations or guidelines.

In countries like USA, Spain, Greece and many more only regional standards exist. In Europe, there are no guidelines or regulations at the European Union level. A very limited number of European countries have guidelines on water reclamation and reuse as i) they usually do not need to reuse water ii) their rivers have adequate dilution factor (Kramer and Post, 2001). EU member states such as Cyprus, France, Greece, Italy, Spain and Portugal have developed the most comprehensive standards specifically for water reuse practices since they suffer from very dry climate. Their water resources are increasingly under stress, leading to water scarcity.

The standards for physical-chemical parameters stated in the Table 10 reflect the requirements stated by US EPA and few EU states that have developed comprehensive standards based on European Directives such as Directive 91/271/EEC on the quality of treated effluent disposal and Directive 2008/105/EC on environmental quality standards and emission limits. The standards for microbiological parameters are according to the WHO guidelines for the safe use of wastewater in agriculture and aquaculture and US EPA for applications such as aquifer recharge and irrigation of golf courses (Sanz and Gawlik, 2014).

Table 10 Reclaimed water quality guidelines depending on specific use according to US EPA, EU and WHO;

Source- Kramer and Post,2001; US EPA, 2012; Salgot et al., 2005; Sanz and Gawlik, 2014

Parameter	US-EPA	As per (91/271/EEC) directive and WHO	EC treated water quality
<b>pH</b>	6-9.5 <sup>a-e</sup>	6-9.5 <sup>a-e</sup>	7-8
<b>TSS (mg/L)</b>	30 <sup>a-e,k,l</sup>	≤ 10 <sup>j,k,l,h</sup>	≤ 10
<b>COD (mg/L)</b>	70-100 <sup>a-h,k,l</sup>	< 70 <sup>a,e,h,k,l</sup>	< 30
<b>Total P (mg/L)</b>	-	0.2-5 <sup>a,d,e,h</sup>	0-0.3
<b>Turbidity (NTU)</b>	-	≤ 5 NTU <sup>i,k,l</sup>	4-8 NTU
<b>TN (mg/L)</b>	-	< 15	< 3
<b>Fe (mg/L)</b>	2 <sup>a,d,g,h</sup>	2 <sup>a,d,g,h</sup>	5
<b>Fecal coli (cfu/100ml)</b>	≤ 200 <sup>a-e</sup>	< 20 <sup>a,d</sup> , ≤ 1000 <sup>a,j,h,k,l</sup>	14
<b>C. perfringens spores (cfu/ml)</b>	<1 <sup>d</sup> , < 10 <sup>d,k</sup>	<1 <sup>i,d,e,l</sup> , < 10 <sup>b,c,h,k</sup>	< 1
<b>Somatic coliphages (pfu/L)</b>	< 1 <sup>k,l</sup>	< 1 <sup>l</sup> < 1000 <sup>a,d</sup>	Below detection limit as per ISO 10705-2:2000

(a)-Restricted access area irrigation, (b)-Agricultural reuse-food crops commercially processed, (c)- Agricultural use non-food crops, (d)-Landscape impoundments where public contact with reclaimed water is not allowed, (e)- Environmental reuse, (f)- Construction reuse, (g)-Industrial reuse, (h)- Recirculating cooling towers, (i)-food consumed raw, (j)-food consumed raw without skin, (k)-Aquifer recharge, (l)- Residential use, toilet flushing.

The batch study results of EC obtained at high charge dosage of 400 C/L shows that the treated water quality abides by the reclaimed water quality regulations. In terms of microbiological quality, the water can be used for restricted access irrigation, direct aquifer recharge, for landscape impoundments where reclaimed water is not in direct contact with the public, for residential use and toilet flushing. The physical and chemical water quality enhances reuse scope in irrigation for commercially processed food crops, restricted irrigation, aquifer recharge and many more. Further optimization of the treatment and addition of enhanced settler with sand filtration can further improve the water quality and widen the scope for reuse.

## Chapter-5

### Discussion

#### 5.1 pH increase during electrocoagulation

The pH increase with increasing charge dosage was associated with the release of  $\text{OH}^-$  at the cathode and  $\text{Fe}^{2+}$  at the anode which did not bind with  $\text{OH}^-$ , thus resulting in excess concentration in the bulk solution.

Alongside, the pH increased at high CDR similar to previous studies by Holt et al., 2002 and Dubrawski and Mohseni, 2013. This phenomenon was due to the faster generation of  $\text{Fe}^{2+}$  and  $\text{OH}^-$  species at high CDR within a short span of an active electric field. This limitation in time reduced the mass transfer of cathodically generated  $\text{OH}^-$  towards the anode, allowing excess concentration in the bulk solution and increasing the pH. High current intensity due to high CDR increased  $\text{Fe}^{2+}$  flux ( $\text{mol/m}^2/\text{sec}$ ), allowing excess concentrations near the anode and driving hydrolysis further to the formation of ferrous hydroxide.

As  $\text{Fe}^{2+}$  was converted to  $\text{Fe}^{3+}$  at alkaline pH and  $\text{OH}^-$  was no longer released in the wastewater, the oxidizing conditions decreased the pH close to the initial value as  $\text{Fe}^{3+}$  bound to  $\text{OH}^-$  to form ferric hydroxides. However, the final pH depended on low alkalinity, buffering capacity of wastewater and solubility of specific  $\text{Fe}^{2+}$  and  $\text{Fe}^{3+}$  compounds produced.

#### 5.2 Reason for a high Faradic Efficiency

The experimental mass of iron released during the experiment with real wastewater effluent was observed to be 14-20% higher than the theoretical mass predicted by Faraday's law. This atypical faradic yield of iron species can be due to several possibilities such as anomalous pitting corrosion behavior of iron and rapid oxidation of oxide film formed on the electrode surface (Khaled et al., 2014; Secula et al., 2012). These electrochemical dissolutions can produce iron hydroxides and hydrogen bubbles greater than the amount that is expected to be produced at the anode and cathode respectively.

Similarly, anodic oxidation of iron simultaneously leads to the formation of  $\text{Fe}^{2+}$  and  $\text{Fe}^{3+}$ . A previous study reported 20% of the total electrode mass to be dissolved by chemical dissolution and the

remaining 80% by electrochemical dissolution (Singh and Ramesh, 2013). This valence difference created by chemical and electrochemical dissolution directly affects the calculated theoretical mass of iron (Secula et al., 2012) (Khaled et al., 2014).

### **5.3 Influence of charge dosage rate**

The direct influence of charge dosage over current density on pollutant removal is observed during the investigation. The decrease in concentration of physical, chemical and biological parameters with increasing charge dosage (from 10 to 400 C/L) specifies that the removal is governed by excess formation of iron hydroxides during the process.

The previous study by Amrose et al., (2013) demonstrated CDR to control the average contact time between a given iron hydroxide particulate and pollutant in wastewater. At a low CDR, the given time increment has a higher pollutant to iron hydroxide precipitate ratio and a charge dosage increment has a longer average contact time with the pollutant (i.e., amount of pollutant adsorbed per mg of Fe precipitate). This theory is practically observed in the current study with high bacteria attenuation in all three water matrices at high charge dosage and low CDR, allowing higher adsorption onto the flocs with longer contact time. Despite these advantages, the real decision to choose the optimal CDR will also involve the energy cost for each configuration as it can vary for the same charge dosage depending on CDR.

The effect of CDR on treatment time is contradictory to prior literature identifying current density as the key variable controlling minimum treatment time. Current density can easily appear to control treatment time if the volume of wastewater used and the active electrode area are maintained constant throughout all tests. In this case, a change in current density is equivalent to a change in CDR, confounding the effect of two variables (Amrose et al., 2013). For EC reactor designers and practitioners who rarely consider a constant effective electrode area and volume across reactors, CDR, and not current density, is the most precise and applicable scaling parameter in determining treatment time.

Additionally, intermediate and high CDRs of 36 and 72 C/L/min resulting in high current and voltage increases the production rate of hydrogen gas which benefits pollutant removal by floatation. A high current (>1 A) used at high CDR is observed to be effective, avoids delay and produces oxidant and disinfecting species (Kourdali et al., 2018). In addition, literature shows that a high CDR leads to the transfer of a non-settleable fraction into a settleable fraction depending on the formation of microscopic gas bubbles near the electrodes (Pouet and Grasmick et al., 1995). This conduct can be

associated with a relatively high reduction of COD and organic N concentrations in this study at 36 C/L/min in real wastewater effluent. To validate the mechanism of floatation, this study can be further extended to bubble-particle interaction depending on the surface properties (hydrophobicity) of the pollutants.

The previous study by Ricordel et al., (2010) demonstrated CDR to vary the fluid regime in the system along with determining the bubble production rate. In this study, a low CDR and current of 7.2 C/L/min and 0.12 A respectively instigated a low hydrogen bubble density, allowing a low upward momentum flux causing poor mixing within the beaker. Under these conditions, sedimentation of flocs was more efficient than floatation. Whereas, at high CDR and current of 36 C/L/min and 0.6 A respectively, the bubble density allowed stronger mixing to favor floatation over sedimentation. This mixing rate also influenced the collision between the particles, floc growth, and fluid regime which varied the floc structures. At 36 and 72 C/L/min, smaller flocs with a compact structure and stable particle size distribution were observed similar to the study by Lee, (2015). These smaller flocs are produced when the floc aggregation and breakage balance to create flocs with a limited size due to effective mixing.

In the study with real wastewater effluent, the variation in pollutant reduction at low and high CDR demonstrates the effect of sedimentation and floatation mechanisms. The removal of enteric bacteria indicators and somatic coliphages is relatively high at 7.2 C/L/min whereas reduction of *C. perfringens* spores, TN and COD are higher at 36 C/L/min. These observations might indicate that the improved removal efficiency at 36 C/L/min is by the combined effect of floc floatation and sedimentation.

#### **5.4 Proposed removal mechanisms for enteric pathogen indicators and ARB**

The goal of this study was to assess the effect of Fe-EC on the attenuation of enteric pathogen indicators and ARB in municipal wastewater effluent, along with evaluating the system in controlled settings using model indicators such as WR1 *E. coli* and  $\phi$ X174 Somatic coliphages in demi water and synthetic wastewater effluent. The two model indicators performed very differently in the presence and absence of wastewater quality parameters. WR1 *E. coli* attenuation was the highest in demi water, which was void of any wastewater parameters, followed by synthetic and real wastewater effluent. Whereas,  $\phi$ X174 Somatic coliphages removal was very poor in demi-water but improved drastically in synthetic and real wastewater effluent indicating the role of particle attachment and enmeshment with wastewater parameters.

The highest removals achieved in demi water and synthetic wastewater effluent do not represent the treatment effectiveness in a real wastewater matrix but confirms the capability of Fe-EC on microbial

attenuation in water matrices without complex water quality parameters such as treatment of shallow groundwater with fecal contamination.

#### **5.4.1 *E.coli*, Enterococci, ESBL *E.coli* and VRE**

The investigation with real wastewater effluent exhibited effective attenuation of *E. coli*, Enterococci, *ESBL E.coli* and VRE with increasing charge dosage from 50 to 400 C/L. Similar removal of all four indicators irrespective of their different cell wall compositions coincide with the previous study by Delaire et al., (2016). This similarity is associated with the phosphate functional groups (mainly on teichoic acids and on phospholipids) present abundantly on Gram-positive and Gram-negative bacteria (Borrok et al., 2005) which form the primary binding sites for EC precipitates. The main removal pathways contributing to bacteria attenuation are i) physical removal by adhesion of EC precipitates onto bacterial cell walls, and ii) inactivation by reactive species produced during Fe(II) oxidation by  $O_2$  (Delaire et al., 2016). This study did not focus on Electro-Fenton process releasing Fenton reagents that can inactivate the bacteria or improve the oxidation of organic compounds present in the wastewater or use high current intensities beyond 1A to damage bacterial cell wall. Since Fenton production of reactive oxygen species was not a part of this study and similar observations by Delaire et al., (2016) demonstrated the effect of Fenton like reactions is negligible at current below 1A. This directed the main attenuation mechanism towards physical removal by adsorption onto the flocs.

Literature shows mechanisms such as double-layer compression and charge neutralization to be prominent with unstable Fe species like  $FeOH^+$ ,  $Fe(OH)_2(s)$  and  $FeO_2^{2-}$  which can be converted to amorphous hydroxide precipitates through series of hydrolysis processes. Whereas, other mechanisms such as adsorption, charge neutralization and entrapment are prominent with stable species such as  $Fe_2O_3$  (Hematite),  $Fe_3O_4$  (magnetite) and  $\alpha Fe^{3+}O(OH)$  (goethite) (Li et al., 2017). The formation of goethite at 400 C/L in real wastewater effluent might indicate adsorption, charge neutralization and entrapment to be mainly responsible for bacteria abatement.

Modelling removal kinetics shows a linear relationship between bacteria reduction and iron dosing. A slightly higher rate constant at 7.2 C/L/min compared to 36 C/L/min indicates the effect of slow iron dosing thus improving contact time between the iron precipitates and bacteria. At 36 C/L/min the coagulant is dosed at a faster rate which might cut-down the sufficient time but the efficient mixing due to excess  $H_2$  gas produced can improve entrapment within the flocs during flocculation phase. However, further studies must focus on improving flocculation, studying floc characteristics at varying CDRs which can aid better pollutant abatement.

#### **5.4.2 *Clostridium perfringens* spores**

The spores were effectively removed in this study compared to previous study by Estrada et al., (2017). The spores contain carboxyl functional group which forms the major negatively charged point on their surface (Bustamante et al., 2001). As a result, these groups possess a strong affinity with the ferric ions especially in the pH range of 4-8. The physical removal is attributed to sweep coagulation. The removal of 2.7 log units by EC, which is higher than 1-2 log removal units by conventional chemical coagulation (LeChevallier and Au, 2004) demonstrates the effectiveness of EC.

However, the removal trend of spores was very different from that of bacteria and coliphages. A linear removal was observed until charge dosage of 100-200 C/L beyond which tailing was seen. An increased iron dosage does not seem to affect the removal beyond a certain concentration. Though the rate constant at 7.2 C/L/min is higher than 36 C/L/min, the efficient mixing might have increased the reduction in spores beyond 200 C/L (at high CDR) letting them to better sweep along with the flocs during settling.

#### **5.4.3 Somatic coliphages**

Removal of Somatic coliphages was similar to the studies by Estrada et al., (2017) and Heffron et al., (2019). As per literature, the isoelectric point of Somatic coliphages is near neutral (6-7) as a result, it is more likely to destabilize and aggregate due to charge neutralization at pH 7, which contributes to physical removal at circumneutral pH (Heffron et al., 2019). The removal achieved in this study is likely higher than 2.7 log units, which is similar to the removal achieved in chemical coagulation (2-3 log units) (LeChevallier and Keung Au, 2004). The removal rate constants are similar at both CDRs indicating destabilization of coliphages by iron precipitates produced in equal quantity at both the rates.

### **5.5 Proposed removal mechanisms for wastewater quality parameters**

In addition to effective removal of enteric pathogen indicators and ARB, the concentration of phosphorous, COD and true color significantly reduced in treated real wastewater effluent.

Phosphorous removal was similar and effective in both synthetic and real wastewater effluent. Associating with the removal mechanisms observed in previous studies, reduction of P in this study is due to adsorption on  $\text{Fe}^{3+}$  hydrolysis species and by  $\text{Fe-OH-PO}_4^{3-}$  complexes. In case such complexes were formed in the sludge, they could not be detected using XRD analysis as they may lack a

crystalline structure. Due to a very strong affinity between P and iron flocs, their removal seemed to be unaffected with varying CDRs.

TN reduction monitored in both synthetic and real wastewater effluents were dissimilar to each other. Literature shows that the N source urea used in synthetic wastewater effluent is prone to electrochemical oxidation to produce  $N_2$  and  $CO_2$  (Urbanczyk et al., 2016). Oxidation of species is controlled by the dissolved oxygen (DO) concentration in wastewater. During EC,  $Fe^{2+}$  oxygenation and cathodic reduction cause depletion in DO over time (with increasing charge dosage). The effect of this is evident in synthetic wastewater effluent, with the highest reduction in N concentration at 10 C/L (start of the process) and a gradual increase in concentration with increasing charge dosage up to 200 C/L. This means that a decrease in DO hampers oxidation of urea thus lowering its removal with increasing treatment time.

Whereas, TN removal in real wastewater effluent was not effective. Quantifying the removal efficiency of organic and inorganic N separately showed maximum removal of organic N. Decrease in  $NO_3^-$  concentration was a result of the electrochemical reduction to  $NH_4^+$  and  $NO_2^-$ , thus increasing their concentrations. A high CDR of 36 C/L/min demonstrated the effect of high current in increasing bubble generation rate, resulting in more efficient and faster removal of organic N as observed by Li et al., (2010).

The COD reduction in real wastewater effluent indicates the removal of organic molecules having  $OH^-$  groups that adsorb onto  $Fe^{3+}$  precipitates to form insoluble compounds. Another possibility is that the microscopic bubbles released due to hydrogen gas transfer a non-settleable fraction into a settleable fraction, hence aiding their reduction. However, in this study, a difference in COD reduction at low and high CDR was not observed to attribute the result to the formation of gas bubbles.

Since TSS and turbidity concentrations were very low in real wastewater effluent (before treatment), the effectiveness of EC was not clearly exhibited. But previous studies carried out with high concentrations in raw municipal and tannery wastewater have shown EC to aid 70-80% of removal. Post-treatment their concentration increased (considering their low initial concentration) due to the production of metallic species, hydroxides and carbonates during EC. However, aggregation of excess Fe precipitates at high charge dosages of 200 and 400 C/L can sweep coagulate these dispersed particles and sediment thus reducing their concentration.

Another possibility is due to dosing of excess coagulants (higher than required to remove a certain turbidity concentration) which can cause restabilization of colloids and metal ions by reversing their

charge. If charge reversal takes place, it will decrease the removal efficiency of other pollutants and this is clearly not the case in this study as seen from the results. Hence, the increase in TSS and turbidity can relate to the addition of metallic species and hydroxides and not to restabilization of colloids or metallic species.

Presence of minute insoluble hydroxide particles in the supernatant which are hard to settle contributed to apparent color, which can be categorized as turbidity. These particles can be eliminated by filtering the samples to witness true color. A higher reduction at 36 C/L/min coincides with a higher reduction of TSS and turbidity at the same rate. These results suggest the need for an enhanced settling right after EC to settle the produced Fe precipitates followed by a sand filtration to remove the residual particles dispersed in the supernatant. The filtration step is necessary to improve the overall quality of the treated effluent.

The treated effluent quality lies within the reclaimed water quality guidelines stated by the international organizations such as WHO, US EPA which increases the scope of implementing EC for secondary wastewater effluent polishing in the existing treatment train with further much-needed research.

## Chapter-6

### Conclusion

The aim of this study was to assess the performance of low voltage iron electrocoagulation to remove enteric pathogen indicators and antibiotic-resistant bacteria for an eventual water reuse scheme. The highest removal of pathogen indicators was observed at charge dosage of 400 C/L and charge dosage rate of 7.2 C/L/min after overnight settling. The marginally higher microbial removal rate at low CDR (7.2 C/L/min) was due to the longer contact time between micro-organism and coagulant. Alongside, effective removal of phosphorous, COD and true color was observed at the same charge dosage of 400 C/L. The excess hydrogen gas released at high CDR of 36 C/L/min increased the removal of COD, TN by floatation and effective mixing enhanced pollutant encapsulation during flocculation. However, the supernatant still contained minute insoluble hydroxide particles which were difficult to settle. Hence, installation of a sedimentation tank immediately after EC is suggested for enhanced settling, followed by a sand filter to remove the dispersed colloids and improve the overall effluent quality.

The experiments conducted under various conditions exhibited contaminant removal to be increased with increasing charge dosage i.e., the amount of iron generated. The produced flocs were separated by sedimentation at low CDR of 7.2 C/L/min but the increased bubble generation rate at high CDRs of 36 and 72 C/L/min led to the separation by floatation. Observing the role of charge dosage and CDR in influencing pollutant removal and determining treatment duration (even at varying volume and electrode area), they can be addressed as the key scaling parameters which could be used by practitioners and in the designing of EC reactors.

The effective treatment of real wastewater effluent was achieved at charge dosage of 400 C/L with an operating cost of 0.17 €/m<sup>3</sup> at 7.2 C/L/min and 0.55 €/ m<sup>3</sup> at 36 C/L/min. The treatment cost of 0.17 €/m<sup>3</sup> compared with alternative technologies like UV, ozone, activated carbon and reverse osmosis showed EC to be a feasible and cost-efficient tertiary treatment option. With further investigations to scale-up, this technology can be fully developed into an effective, low cost, decentralized/centralized treatment system.

The treated water quality produced at charge dosage of 400 C/L was within the prescribed guidelines of WHO, USEPA and comprehensive standards developed by few EU member states for reclaimed water use for specific purposes. The delivered water quality offers scope for use in restricted access area irrigation, aquifer recharge, in agriculture for commercially produced food crops, landscape impoundments, industrial cooling, residential use and toilet flushing. However, a health risk assessment, based on hazard calculations must be performed before assigning the reclaimed water for any of the above-mentioned purposes.

## Chapter-7

### Recommendations

1. Based on the results of this research, several new questions were raised while some remain unanswered. A CDR of 7.2 C/L/min was observed to be effective for high removal of enteric pathogen indicators and ARB but, increasing CDR though shortened the treatment time increased the electricity consumption. Further research can be conducted varying the CDR between 7.2 and 36 C/L/min to identify the suitable rate depending on the purpose of treatment and secondary effluent quality to achieve refined water quality.
2. Further study should be focussed on improving floc formation that can enhance the removal efficiency. A suitable CDR between 5-36 C/L/min which provides optimum mixing velocity to form large macro flocs must be investigated.
3. Study of flocs particle size distribution under varying charge dosage rates is necessary to understand aggregation mechanisms.
4. Study to distinguish removal mechanism in microbial mitigation - inactivation and physical removal by elution technique as performed by Heffron et al., (2019) must be conducted.
5. A representative pilot plant experiment should be conducted suitably in a batch mode or continuous mode coupling with a settler and sand filter which will be beneficial in incorporating treatment conditions to a full-scale plant.
6. Faradic efficiency (FE) can reduce during continuous operation and reduce treatment efficiency. Also, the formation of surface layers is often stated as a disadvantage of EC. For this purpose, field studies investigating long-term FE at different CDRs and secondary effluent quality must be tested. Further, the effect of high or low CDR in increasing FE must be tested.
7. The treatment efficiency and cost can still be improved by changing certain design parameters. For example, electrode arrangement can be tested for monopolar and bipolar connection modes, increasing the stirring speed while maintaining a low CDR which can enhance bubble formation.

8. EC process generates iron sludge as residual. In this study, goethite was detected after treating real wastewater effluent at 400 C/L. Goethite was observed to be attracted by a magnet and literature confirms the existence of magnetic properties in natural goethite (Dekkers, 1988). Based on this observation, future research can be focused on pelletizing iron sludge which can be used as adsorbents for the removal of heavy metals, arsenic and micropollutants to name a few that have an affinity with iron precipitates.
9. A health risk assessment for treated water based on the requirement of reuse application such as irrigation, domestic use and many more must be performed with the data from pilot-scale setup.

## References

- Abbas, S. H., Ali W. H. (2018). Electrocoagulation technique used to treat wastewater: A Review. *American Journal of Engineering Research*, Vol 7, 74-88.
- Abudalo, R. A., Ryan, J. N., Harvey, R. W., Metge, D. W., & Landkamer, L. (2009). Influence of organic matter on the transport of *Cryptosporidium parvum* oocysts in a ferric oxy-hydroxide-coated quartz sand saturated porous medium. *Water Research*, 44(4), 1104-1113
- Alcalde-Sanz, L., & Gawlik, B. M. (2017). Minimum quality requirements for water reuse in agricultural irrigation and aquifer recharge. *Towards a Legal Instrument on Water Reuse at EU Level*.
- Al-Shannag, M., Bani-Melhem, K., Al-Anber, Z., & Al-Qodah, Z. (2013). Enhancement of COD-nutrients removals and filterability of secondary clarifier municipal wastewater influent using electrocoagulation technique. *Separation Science and Technology*, 48(4), 673-680.
- American Public Health Association., American Water Works Association., & Water Environment Federation. (1998). *Standard methods for the examination of water and wastewater*. Washington, D.C: APHA-AWWA-WEF.
- Amrose, S., Gadgil, A., Srinivasan, V., Kowolik, K., Muller, M., Huang, J., & KostECKI, R. (2013). Arsenic removal from groundwater using iron electrocoagulation: effect of charge dosage rate. *Journal of Environmental Science and Health, Part A*, 48(9), 1019-1030.
- Anfruns-Estrada, E., Bruguera-Casamada, C., Salvadó, H., Brillas, E., Sirés, I., & Araujo, R. M. (2017). Inactivation of microbiota from urban wastewater by single and sequential electrocoagulation and electro-Fenton treatments. *Water Research*, 126, 450-459.
- Aoudj, S., Khelifa, A. & Drouiche, N., 2017. Removal of fluoride, SDS, ammonia and turbidity from semiconductor wastewater by combined electrocoagulation-electroflotation. *Chemosphere*, Issue 180, pp. 379-387
- Bayar, S., Yıldız, Y. Ş., Yılmaz, A. E., & İrdemez, Ş. (2011). The effect of stirring speed and current density on removal efficiency of poultry slaughterhouse wastewater by electrocoagulation method. *Desalination*, 280(1-3), 103-107.
- Bani-Melhem, K.; Elektorowicz, M. (2011) Performance of the submerged membrane electro-bioreactor (SMEBR) with iron electrodes for wastewater treatment and fouling reduction. *J. Member. Sci.*, 379: 434–439.
- Boudjema, N., Drouiche, N., Abdi, N., Grib, H., Lounici, H., Pauss, A., & Mameri, N. (2014). Treatment of Oued El Harrach river water by electrocoagulation noting the effect of the electric field on microorganisms. *Journal of the Taiwan Institute of Chemical Engineers*, 45(4), 1564-1570.

- Bukhari, A.A., Abuzaid, N.S., Abdulappa, M.K., Essa, M.H. 1999. Pretreatment of domestic wastewater in an electrochemical cell. In: The Fifth Saudi Engineering Conference, vol. 3
- Bukhari, A. A. (2008). Investigation of the electrocoagulation treatment process for the removal of total suspended solids and turbidity from municipal wastewater. *Bioresource technology*, 99(5), 914-921.
- Bui, X. T., Vo, T. P. T., Ngo, H. H., Guo, W. S., & Nguyen, T. T. (2016). Multicriteria assessment of advanced treatment technologies for micropollutants removal at large-scale applications. *Science of the Total Environment*, 563, 1050-1067.
- Bustamante, H. A., Shanker, S. R., Pashley, R. M., & Karaman, M. E. (2001). Interaction between *Cryptosporidium* oocysts and water treatment coagulants. *Water Research*, 35(13), 3179-3189.
- Chahal, C., Van Den Akker, B., Young, F., Franco, C., Blackbeard, J., & Monis, P. (2016). Pathogen and particle associations in wastewater: significance and implications for treatment and disinfection processes. In *Advances in applied microbiology* (Vol. 97, pp. 63-119). Academic Press.
- Chen, X., Chen, G.C., Yue, P.L., 2000. Separation of pollutants from restaurant wastewater by electrocoagulation. *Sep. Purif. Technol.* 19, 65–76.
- D'Costa, V. M., King, C. E., Kalan, L., Morar, M., Sung, W. W., Schwarz, C., ... & Golding, G. B. (2011). Antibiotic resistance is ancient. *Nature*, 477(7365), 457.
- De Freitas, J.M.; Meneghini, R. (2001) Iron and its sensitive balance in the cell. *Mutation Res. Founder, Mol. Mech. Mutagen.*, 475: 153–159.
- Dekkers, M. J., 1988. Some rock magnetic parameters for natural goethite, pyrrhotite and fine-grained hematite, *Geologica Ultraiectina* 51, PhD thesis, pp. 219-227, University of Utrecht.
- Delaire, C., van Genuchten, C. M., Amrose, S. E., & Gadgil, A. J. (2016). Bacteria attenuation by iron electrocoagulation governed by interactions between bacterial phosphate groups and Fe (III) precipitates. *Water research*, 103, 74-82.
- Dias, E. H. (2016). *Bacteriophages as surrogates of viral pathogens in wastewater treatment processes*. The University of Brighton.
- Dubrawski, K.L., & Mohseni, M. (2013). Standardizing electrocoagulation reactor design: iron electrodes for NOM removal. *Chemosphere*, 91 1, 55-60 .
- Elimelech, M. (2006). The global challenge for adequate and safe water. *Journal of Water Supply: Research and Technology-AQUA*, 55(1), 3-10.
- Eurostat. (2019, May). *Eurostat*. Retrieved June 29, 2019, from Electricity price statistics: [https://ec.europa.eu/eurostat/statistics-explained/index.php/Electricity\\_price\\_statistics](https://ec.europa.eu/eurostat/statistics-explained/index.php/Electricity_price_statistics)

Fair, R. J., & Tor, Y. (2014). Antibiotics and bacterial resistance in the 21st century. Perspectives in medicinal chemistry, 6, PMC-S14459

Fielding, K. S., Dolnicar, S., & Schultz, T. (2018). Public acceptance of recycled water. *International Journal of Water Resources Development*, 1-36.

Gadgil, A., Amrose, S., Bandaru, S., Delaire, C., Torkelson, A., & van Genuchten, C. (2014). Addressing Arsenic Mass Poisoning in South Asia with Electrochemical Arsenic Remediation. In *Water reclamation and sustainability* (pp. 115-154). Elsevier.

Garcia-Segura, S., Eiband, M. M. S., de Melo, J. V., & Martínez-Huitle, C. A. (2017). Electrocoagulation and advanced electrocoagulation processes: A general review about the fundamentals, emerging applications and its association with other technologies. *Journal of Electroanalytical Chemistry*, 801, 267-299.

Ghernaout, D., Badis, A., Kellil, A. & Ghernaout, B. Application of electrocoagulation in Escherichia coli culture and two surface waters. *Desalination* 219, 118–125 (2008).

Gottschalk, C., Libra, J. A., & Saupe, A. (2009). *Ozonation of water and waste water: A practical guide to understanding ozone and its applications*. John Wiley & Sons

Guidelines for the Safe Use of Wastewater, Excreta and Greywater; World Health Organization: Geneva, Switzerland, 2006.

Heffron, J., McDermid, B., Maher, E., McNamara, P. J., & Mayer, B. K. (2019). Mechanisms of virus mitigation and suitability of bacteriophages as surrogates in drinking water treatment by iron electrocoagulation. *Water research*, 163, 114877.

Holt, P. K., Barton, G. W., Wark, M., & Mitchell, C. A. (2002). A quantitative comparison between chemical dosing and electrocoagulation. *Colloids and Surfaces A: Physicochemical and Engineering Aspects*, 211(2-3), 233-248.

Hong, K. H., Kim, W. Y., Son, D. J., Yun, C. Y., Chang, D., Bae, H. S., & Kim, D. G. (2014). Characteristics of organics and nutrients removal in municipal wastewater treatment by electrolysis using a copper electronic conductor. *Int. J. Electrochem. Sci*, 9, 3979-3989.

ISO, “ISO 10705-2: Water Quality—Detection and Enumeration of Bacteriophages—Part 2: Enumeration of Somatic Coliphages,” International Organisation for Standardisation, Geneva, 2000.

ISO, “ISO 9308-1: 2014 - Water quality -- Enumeration of Escherichia coli and coliform bacteria -- Part 1: Membrane filtration method for waters with low bacterial background flora,” International Organisation for Standardisation, Geneva, 2014.

Jekel, M. R. (1986). The stabilization of dispersed mineral particles by adsorption of humic substances. *Water Research*, 20(12), 1543-1554.

- Jofre, J., Lucena, F., Blanch, A., & Muniesa, M. (2016). Coliphages as model organisms in the characterization and management of water resources. *Water*, 8(5), 199.
- Khaled, B., Wided, B., Béchir, H., Elimame, E., Mouna, L., & Zied, T. (2015). Investigation of electrocoagulation reactor design parameters effect on the removal of cadmium from synthetic and phosphate industrial wastewater. *Arabian Journal of Chemistry*.
- Kobyas, M., Can, O. T., Bayramoglu, M. (2003), Treatment of textile wastewater by electrocoagulation using iron and aluminium electrodes, *Journal of Hazardous Materials*, 100, 163.
- Koivunen, J., Siitonen, A., & Heinonen-Tanski, H. (2003). Elimination of enteric bacteria in biological–chemical wastewater treatment and tertiary filtration units. *Water Research*, 37(3), 690-698.
- Kourdali, S., Badis, A., Boucherit, A., Boudjema, K., & Saiba, A. (2018). Electrochemical disinfection of bacterial contamination: Effectiveness and modeling study of E. coli inactivation by electro-Fenton, electro-peroxi-coagulation and electrocoagulation. *Journal of environmental management*, 226, 106-119.
- Kramer, A., Post, J., & Reseach, A. (2001). Guidelines and Standards for Wastewater Reuse. *Adelphi Reseach Berlin*, 1-31.
- Lacasa, E., Canizares, P., Saez, C., Fernández, F. J., & Rodrigo, M. A. (2011). Electrochemical phosphates removal using iron and aluminium electrodes. *Chemical Engineering Journal*, 172(1), 137-143.
- Lakshmanan, D., Clifford, D. A., & Samanta, G. (2009). Ferrous and ferric ion generation during iron electrocoagulation. *Environmental science & technology*, 43(10), 3853-3859.
- LeChevallier, M. W., & Au, K. K. (2004). *Water treatment and pathogen control*. IWA Publishing.
- Levine, A. D., & Asano, T. (2004). Peer-reviewed: recovering sustainable water from wastewater.
- Lee, S. Y. (2015). Investigating the generation efficiency, growth and structure of flocs produced by electrocoagulation.
- Li, X-G.; Cao, H-B.; Wu, J-C.; Yu, K-T. (2001) Inhibition of the metabolism of nitrifying bacteria by direct electric current. *Biotechnol. Letters*, 23: 705–709
- Li, M., Feng, C., Zhang, Z., Yang, S., & Sugiura, N. (2010). Treatment of nitrate-contaminated water using an electrochemical method. *Bioresource technology*, 101(16), 6553-6557.
- Li, N., Sheng, G. P., Lu, Y. Z., Zeng, R. J., & Yu, H. Q. (2017). Removal of antibiotic resistance genes from wastewater treatment plant effluent by coagulation. *Water Research*, 111, 204-212.
- Maier R, IL Pepper, CP Gerba, C.P. 2009. Environmental microbiology: Academic Press.

MEPS. (2019). Retrieved from MEPS - EU CARBON STEEL PURCHASING PRICE INDEX (SPPI): <http://www.meps.co.uk/EU%20price%20index.htm>

Michael, I., Rizzo, L., McArdeall, C. S., Manaia, C. M., Merlin, C., Schwartz, T., & Fatta-Kassinos, D. (2013). Urban wastewater treatment plants as hotspots for the release of antibiotics in the environment: a review. *Water research*, 47(3), 957-995.

Moellering Jr, R. C. (1998). Vancomycin-resistant enterococci. *Reviews of Infectious Diseases*, 26(5), 1196-1199.

Mollah, M. Y., Morkovsky, P., Gomes, J. A., Kesmez, M., Parga, J., & Cocke, D. L. (2004). Fundamentals, present and future perspectives of electrocoagulation. *Journal of hazardous materials*, 114(1-3), 199-210.

Moreno-Casillas, H. A., Cocke, D. L., Gomes, J. A., Morkovsky, P., Parga, J. R., & Peterson, E. (2007). Electrocoagulation mechanism for COD removal. *Separation and Purification Technology*, 56(2), 204-211.

Müller, S., Behrends, T., & van Genuchten, C. M. (2019). Sustaining efficient production of aqueous iron during repeated operation of Fe (0)-electrocoagulation. *Water Research*, 155, 455464.

Murugananthan, M., Bhaskar, G., Raju, G., Prabhakar, S., 2004. Removal of sulfide, sulfate and sulfite ions by electrocoagulation. *Journal of Hazardous Materials B* 109, 37–44.

Nguyen, D. D., Ngo, H. H., Guo, W., Nguyen, T. T., Chang, S. W., Jang, A., & Yoon, Y. S. (2016). Can the electrocoagulation process be an appropriate technology for phosphorus removal from municipal wastewater? *Science of the Total Environment*, 563, 549-556.

Ni'Am, M. F., Othman, F., Sohaili, J., & Fauzia, Z. (2007). Electrocoagulation technique in enhancing COD and suspended solids removal to improve wastewater quality. *Water Science and Technology*, 56(7), 47-53.

Owoseni, M.C.; Olaniran, A.O.; Okoh, A.I. Chlorine Tolerance and Inactivation of *Escherichia coli* recovered from Wastewater Treatment Plants in the Eastern Cape, South Africa. *Appl. Sci.* **2017**, 7, 810.

Omwene, P. I., Kobya, M., & Can, O. T. (2018). Phosphorus removal from domestic wastewater in electrocoagulation reactor using aluminium and iron plate hybrid anodes. *Ecological engineering*, 123, 65-73.

Ou, F., McGoverin, C., Swift, S., & Vanholsbeeck, F. (2019). Near real-time enumeration of live and dead bacteria using a fibre-based spectroscopic device. *Scientific reports*, 9(1), 4807.

Parsons, S. (Ed.). (2004). *Advanced oxidation processes for water and wastewater treatment*. IWA publishing.

- Picozzi, S. C., Casellato, S., Mattia Rossini, G. P., Tejada, M., Costa, E., & Carmignani, L. (2014). Extended-spectrum beta-lactamase-positive *Escherichia coli* causing complicated upper urinary tract infection: Urologist should act in time. *Urology annals*, 6(2), 107.
- Pouet, M. F., & Grasmick, A. (1995). Urban wastewater treatment by electrocoagulation and flotation. *Water science and technology*, 31(3-4), 275-283.
- Pressdee, J. R. (2006). *Integration of membrane filtration into water treatment systems* (Vol. 91103). American Water Works Association.
- Putri, N. F., Suryadarma, P., Zakiyyah, S., & Manguwidjaja, D. (2018, December). Phosphate addition plays an important role in *Escherichia coli* cell attachment under aerobic condition. In *AIP Conference Proceedings* (Vol. 2049, No. 1, p. 020014). AIP Publishing.
- Pulido, Maria Elena, "Evaluation of an Electro-Disinfection Technology as an Alternative to Chlorination of Municipal Wastewater Effluents" (2005). University of New Orleans Theses and Dissertations. 309. <https://scholarworks.uno.edu/td/309>
- Ren, Z., Zhang, L., & Shi, Y. (2016). UV disinfection of *Staphylococcus aureus* in ballast water: Effect of growth phase on the disinfection kinetics and the mechanization at molecular level. *Science China Technological Sciences*, 59(2), 330-336.
- Research, A. M. (2018, October 30). *Antibiotics Market to Reach \$50.37 Bn, Globally, by 2025 at 2.1% CAGR, Says Allied Market Research*. Retrieved February 3, 2019, from Allied Market Research: <https://www.prnewswire.com/news-releases/antibiotics-market-to-reach-50-37-bnglobally-by-2025-at-2-1-cagr-says-allied-market-research-849872970.html>
- Reuse, N. W. (2012). Potential for Expanding the Nation's Water Supply through Reuse of Municipal Wastewater. *Natural Research Council: Washington, DC, USA*.
- Ricordel, C., Darchen, A., & Hadjiev, D. (2010). Electrocoagulation–electroflotation as a surface water treatment for industrial uses. *Separation and Purification Technology*, 74(3), 342-347.
- Salgot, M., Folch, M., & Unit, S. S. (2018). Wastewater treatment and water reuse. *Current Opinion in Environmental Science & Health*.
- Sanz, L. A., & Gawlik, B. M. (2014). Water reuse in Europe, relevant guidelines, needs for and barriers to innovation. *European Commission Joint Research Centre Institute for Environment and Sustainability*.
- Schwartz, T., Kohnen, W., Jansen, B., & Obst, U. (2003). Detection of antibiotic-resistant bacteria and their resistance genes in wastewater, surface water, and drinking water biofilms. *FEMS microbiology ecology*, 43(3), 325-335.
- Searcy, K. E., Packman, A. I., Atwill, E. R., & Harter, T. (2006). Capture and retention of *Cryptosporidium parvum* oocysts by *Pseudomonas aeruginosa* biofilms. *Appl. Environ. Microbiol.*, 72(9), 6242-6247.

- Secula, M. S., Crețescu, I., & Petrescu, S. (2012). Electrocoagulation treatment of sulfide wastewater in a batch reactor: the effect of electrode material on electrical operating costs. *Environmental Engineering & Management Journal (EEMJ)*, 11(8).
- Singh, T. S. A., & Ramesh, S. T. (2014). An experimental study of CI Reactive Blue 25 removal from aqueous solution by electrocoagulation using aluminium sacrificial electrode: kinetics and influence of parameters on electrocoagulation performance. *Desalination and Water Treatment*, 52(13-15), 2634-2642.
- Sproul, O. J. (1980). A critical review of virus removal by coagulation processes and pH modifications. *A critical review of virus removal by coagulation processes and pH modifications*. EPA.
- Sruthi, G., Ahammed, M. M., & Makwana, A. R. (2018). Effect of source water/wastewater quality on bacterial removal during electrocoagulation. *Water Science and Technology*, 77(5), 1460-1468.
- Symonds, E. M., Cook, M. M., McQuaig, S. M., Ulrich, R. M., Schenck, R. O., Lukasik, J. O., ... & Breitbart, M. (2015). Reduction of nutrients, microbes, and personal care products in domestic wastewater by a benchtop electrocoagulation unit. *Scientific reports*, 5, 9380.
- Tanneru, C. T. & Chellam, S. Mechanisms of virus control during iron electrocoagulation – Microfiltration of surface water. *Water Res* 46, 2111–2120 (2012).
- Tectonics, W. (2019). *Water Tectonics*. Retrieved from Water Tectonics: <http://www.watertectonics.com/electrocoagulation/>
- Templeton, M. R., Andrews, R. C., & Hofmann, R. (2008). Particle-associated viruses in water: impacts on disinfection processes. *Critical Reviews in Environmental Science and Technology*, 38(3), 137-164.
- Toze, S. (2006). Reuse of effluent water—benefits and risks. *Agricultural water management*, 80(1-3), 147-159.
- Urbańczyk, E., Sowa, M., & Simka, W. (2016). Urea removal from aqueous solutions—a review. *Journal of Applied Electrochemistry*, 46(10), 1011-1029.
- US Environmental Protection Agency. (2012). Guidelines for Water Reuse (No. EPA/600/R-12/618).
- Victoria, E. P. A. (2002). Disinfection of treated wastewater. *Guidelines for Environmental Management*, 30.
- Voulvoulis, N. (2018). Water reuse from a circular economy perspective and potential risks from an unregulated approach. *Current Opinion in Environmental Science & Health*, 2, 32-45.
- Wade, W. (2002). Unculturable bacteria—the uncharacterized organisms that cause oral infections. *Journal of the Royal Society of Medicine*, 95(2), 81-83.

Walsh, F. (2014, December 11). *Superbugs to kill 'more than cancer' by 2050*. Retrieved February 3, 2019, from BBC: <https://www.bbc.com/news/health-30416844>

World Health Organization (WHO) Water Sanitation and Health.2015. (assessed on 13 December 2018)

Zaleschi, L., Teodosiu, C., Cretescu, I., & Rodrigo, M. A. (2012). A comparative study of electrocoagulation and chemical coagulation processes applied for wastewater treatment. *Environmental Engineering & Management Journal (EEMJ)*, 11(8).

Zhu, B., Clifford, D. A., & Chellam, S. (2005). Virus removal by iron coagulation– microfiltration. *Water Research*, 39(20), 5153-5161.